

Iris Recognition

Part of the content is based on the tutorial by Kevin W. Bowyer



BiDA Lab

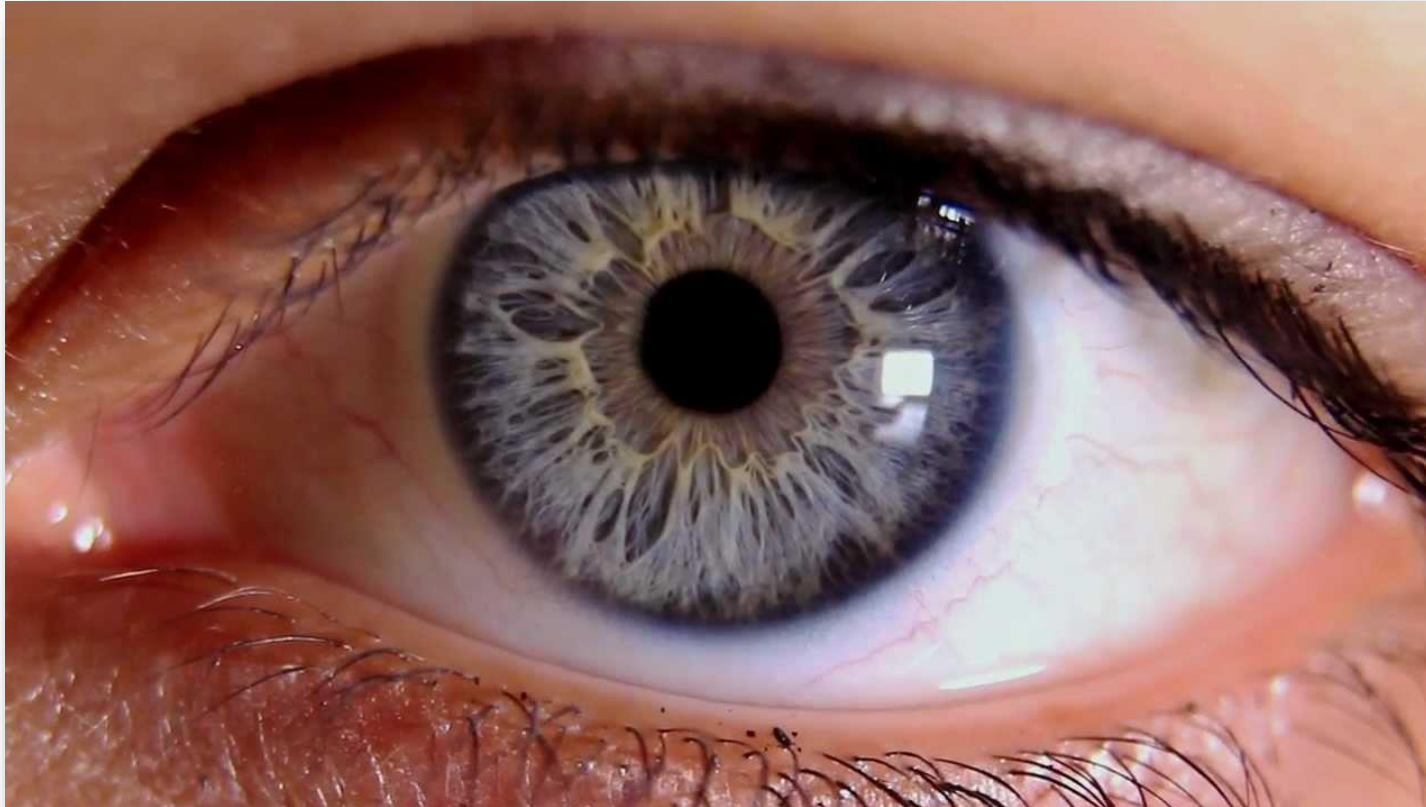
Biometrics & Data Pattern Analytics Lab

UAM

Universidad Autónoma
de Madrid

What is it?

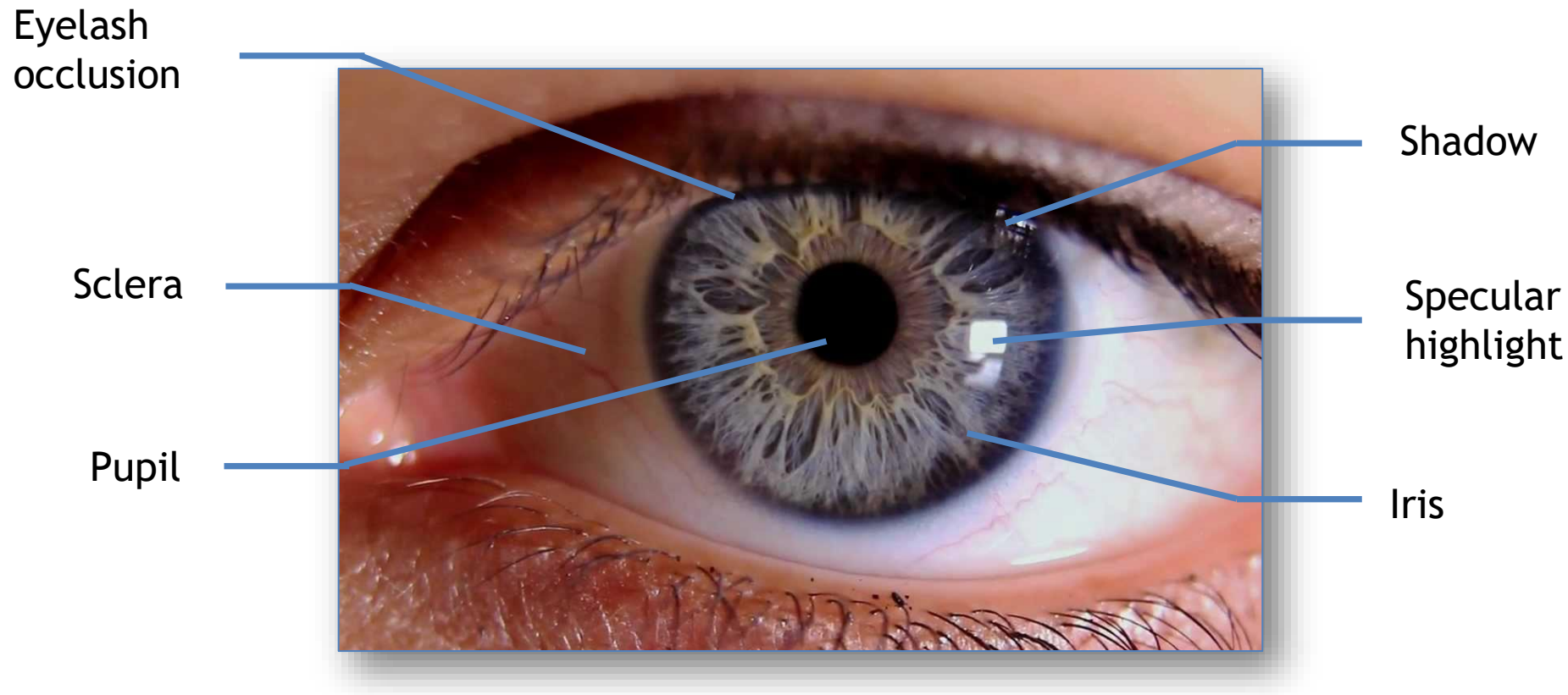
The texture of the iris can be the source of an “iris code” that is unique to that particular iris and is stable across a range of practical imaging conditions.



- K. W. Bowyer and M. J. Burge, *Handbook of iris recognition*. Springer London, 2016.
- J. Daugman, “How iris recognition works,” *IEEE Transactions on Circuits and Systems for Video Technology*, 2004

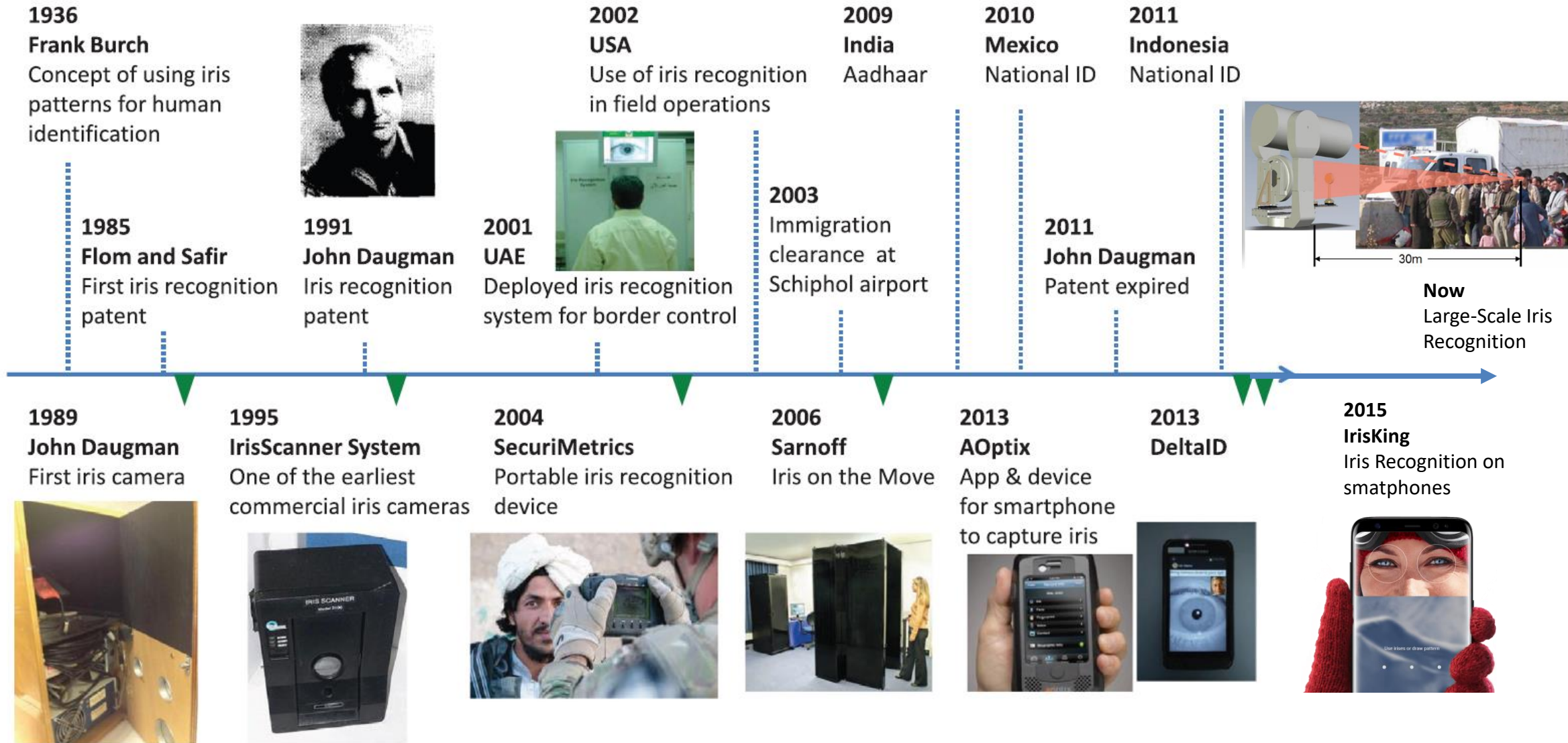
What is it?

The texture of the iris can be the source of an “iris code” that is unique to that particular iris and is stable across a range of practical imaging conditions.



- K. W. Bowyer and M. J. Burge, *Handbook of iris recognition*. Springer London, 2016.
- J. Daugman, “How iris recognition works,” *IEEE Transactions on Circuits and Systems for Video Technology*, 2004

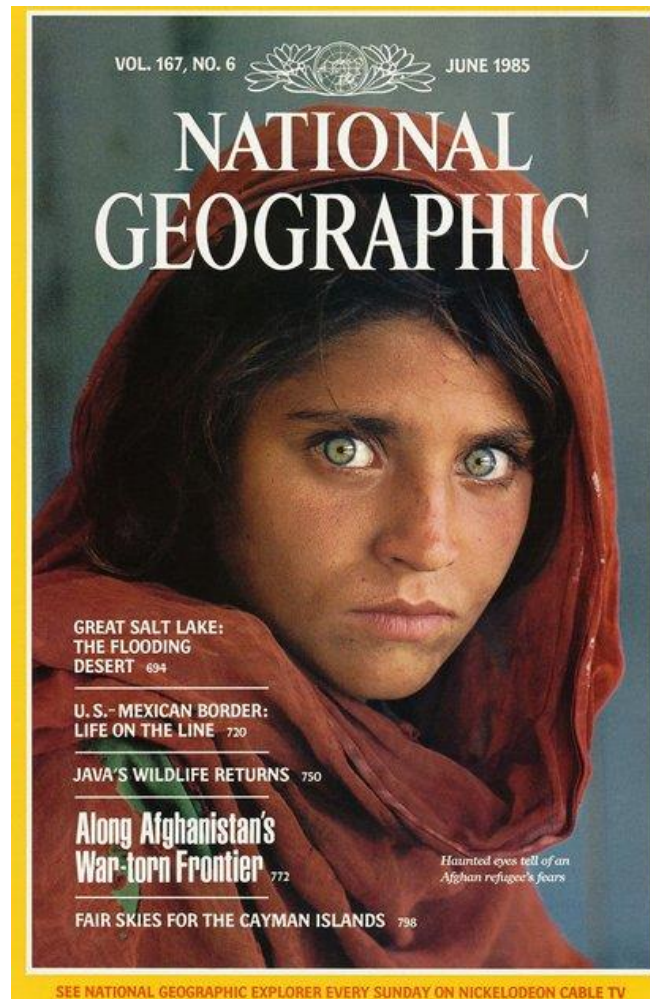
History



- A. K. Jain, K. Nandakumar, and A. Ross, "50 years of biometric research: Accomplishments, challenges, and opportunities." Pattern Recognition Letters, 79, 80-105, 2016.

History

[Sharbat Gula](#): She is an Afghan woman who became famous for her photo taken by the photojournalist Steve McCurry during the Afghan War for the [National Geographic magazine](#).



History

Sharbat Gula: The identity of the girl remained **unknown** for more than 17 years. In January 2002, a National Geographic team was able to find and **identify her using John Daugman iris recognition software.**



History

Sharbat Gula: The identity of the girl remained **unknown** for more than 17 years. In January 2002, a National Geographic team was able to find and **identify her using John Daugman iris recognition software.**



The iris of every human eye has a unique texture of high complexity, which proves to be essentially "immutable" over a person's life. (Daugman, U.S. Patent #5,291,560, 1994.)

History

Aadhaar: It is the world's largest biometric ID System. Each Indian resident has a unique 12-digit identity number based on the **biometric (iris and fingerprint) and demographic data.**

Figures: More than one billion identities.

Goal: Social inclusion enhanced: "To give the poor an identity".



History

Center for Global Development report analyzing India's experience with their Unique ID program.

Conclusions based on data from enrolling 84 million persons.

The Eyes Have It

Iris trumps fingerprints. UID's data suggest that iris scans are far more inclusive than fingerprints, especially when applied to poor populations engaged in heavy manual labor.

They are also more precise for authentication, in terms of having a lower tradeoff curve between errors of acceptance and rejection, even in the best case when the best two fingerprints are known and individually labeled. The rapidly falling price of iris technology

Performance Lessons from India's Universal Identification Program

Alan Gelb and Julia Clark

Abstract

Biometric identification is spreading rapidly across the developing world, where it is helping to close the "identification gap" that separates poor countries from rich ones.

India's Unique Identification (UID) project offers important lessons for other countries. UID's performance data show that large countries can implement biometric ID programs with low levels of exclusion and high accuracy, but this requires the combined use of multiple biometrics.

Center for Global Development
1800 Massachusetts Ave NW
Third Floor
Washington DC 20036
202-416-4000
www.cgdev.org

This work is made available under
the terms of the Creative Commons
Attribution-NonCommercial 3.0
license.

need to allow for failures to enroll and for errors by providing other options to identify and authenticate individuals.

UID's modest cost levels owe much to its standards-based approach, which encourages competition among suppliers and avoids lock-in to proprietary technology. UID also sets standards for the disclosure of performance data which other programs should emulate, and which can be used to help calibrate technology to needs.

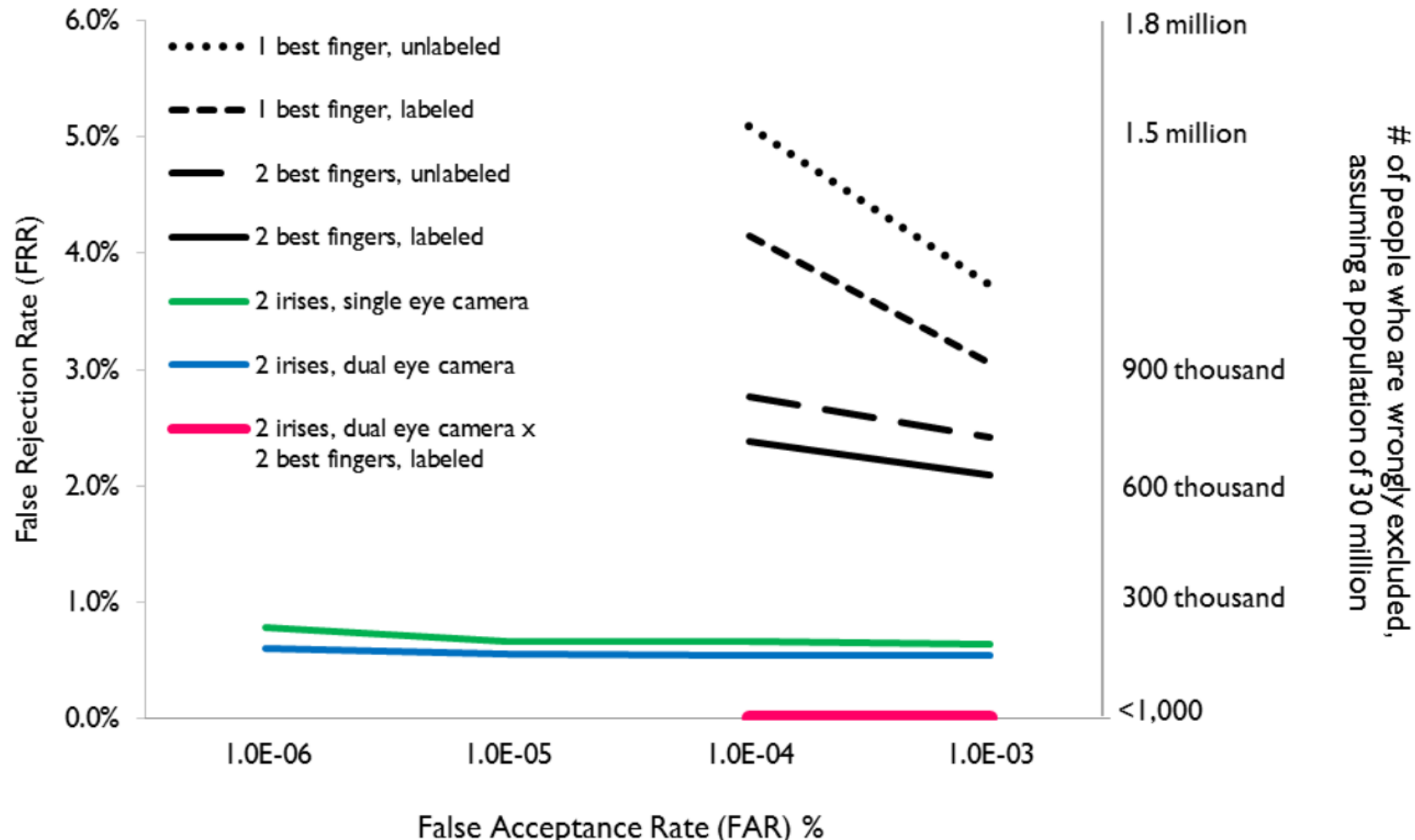
These lessons are also useful for the foreign donors that support many identification systems in poor countries and are concerned that they be both inclusive and effective.

Alan Gelb and Julia Clark. 2013. "Performance Lessons from India's Universal Identification Program." CGD Policy Paper 020. Washington DC: Center for Global Development.
<http://www.cgdev.org/publication/performance-lessons>

CGD is grateful for contributions from the UK Department for International Development in support of this work.

History

Detection Error Tradeoff (DET) of Iris and Fingerprints + Fail to Capture (FTC) Rate



Automatic Iris Recognition: Architecture



Input Iris

Automatic Iris Recognition: Architecture

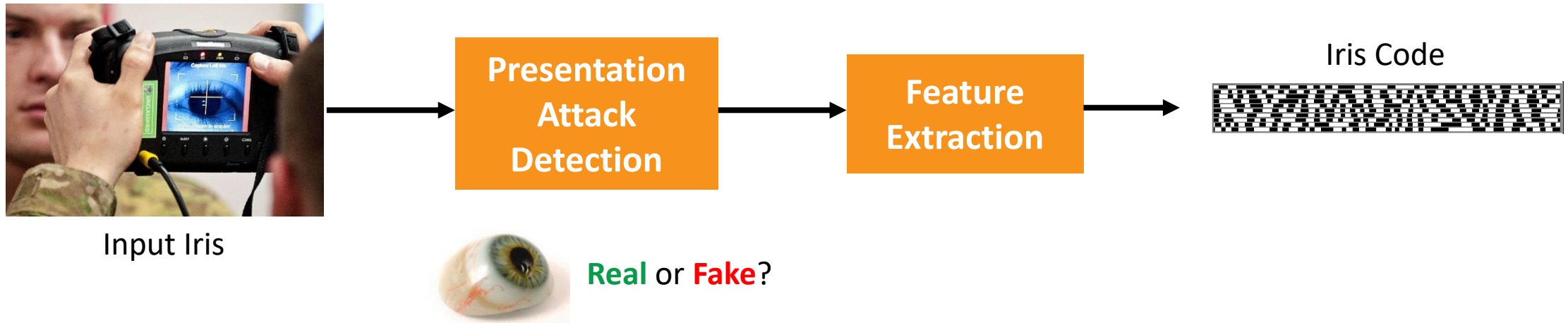


Input Iris

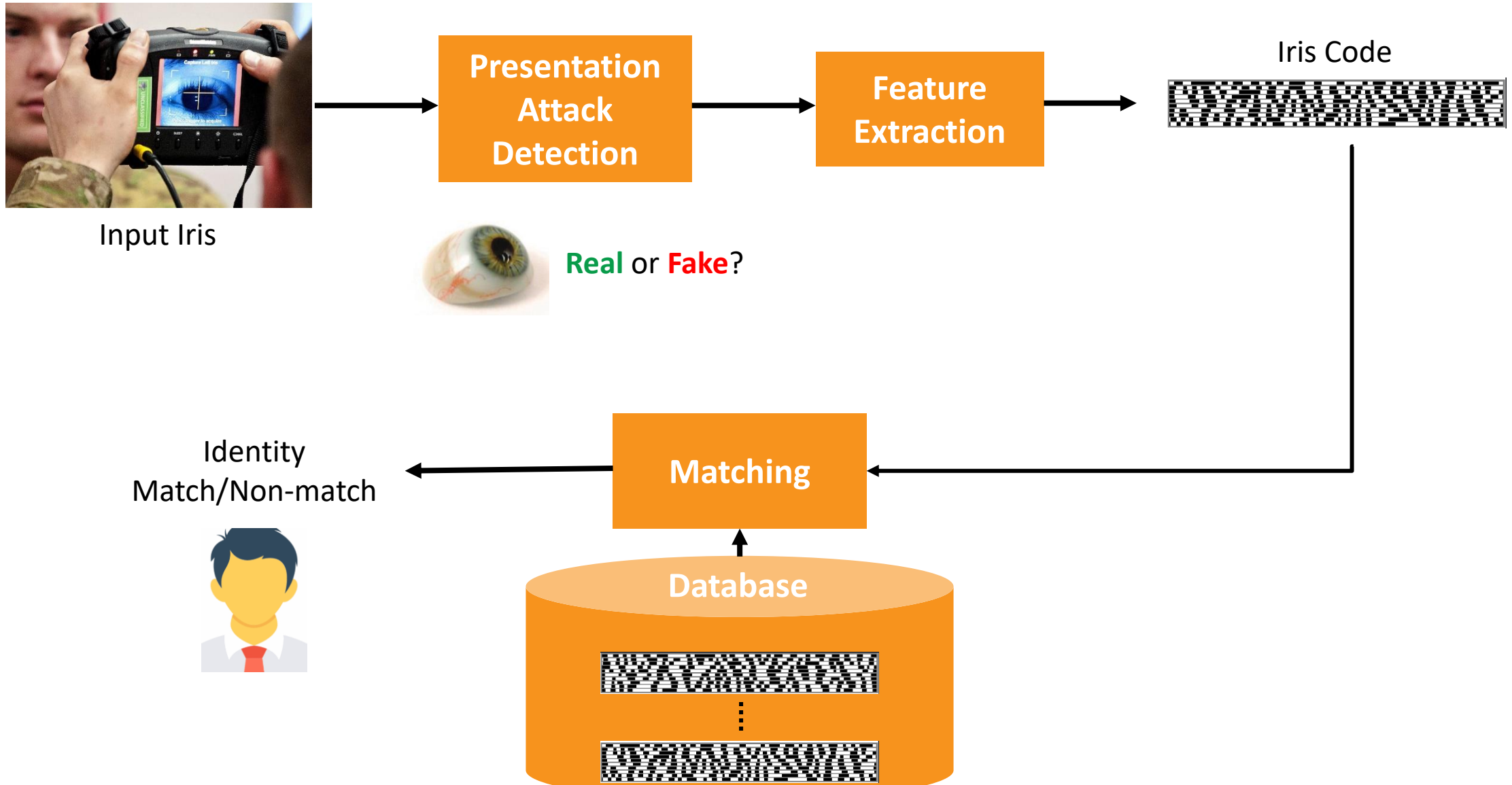


Real or **Fake?**

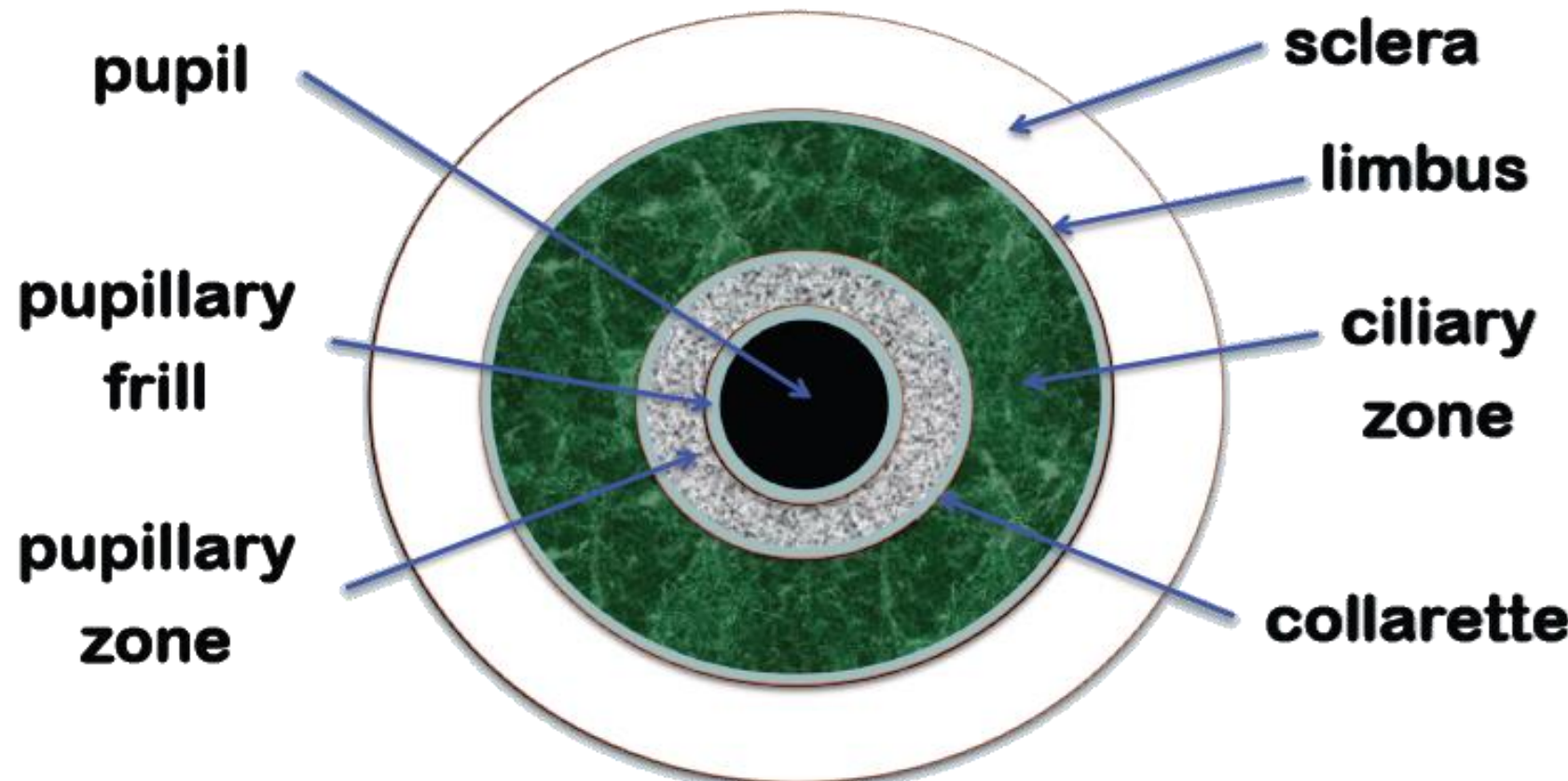
Automatic Iris Recognition: Architecture



Automatic Iris Recognition: Architecture



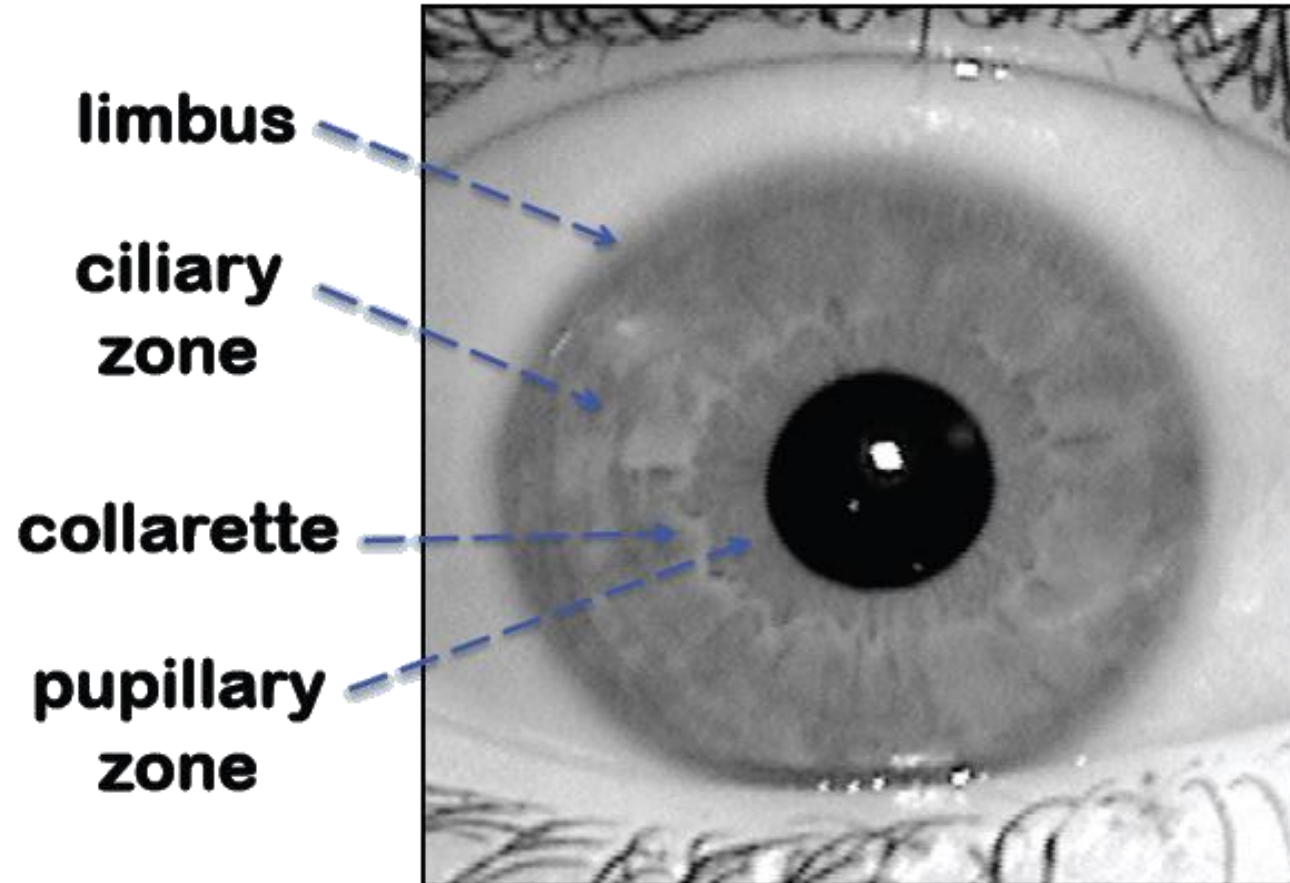
Anatomy of the Iris



front-view diagram of the iris.

- K. W. Bowyer and M. J. Burge, *Handbook of iris recognition*. Springer London, 2016.
- J. Daugman, "How iris recognition works," *IEEE Transactions on Circuits and Systems for Video Technology*, 2004

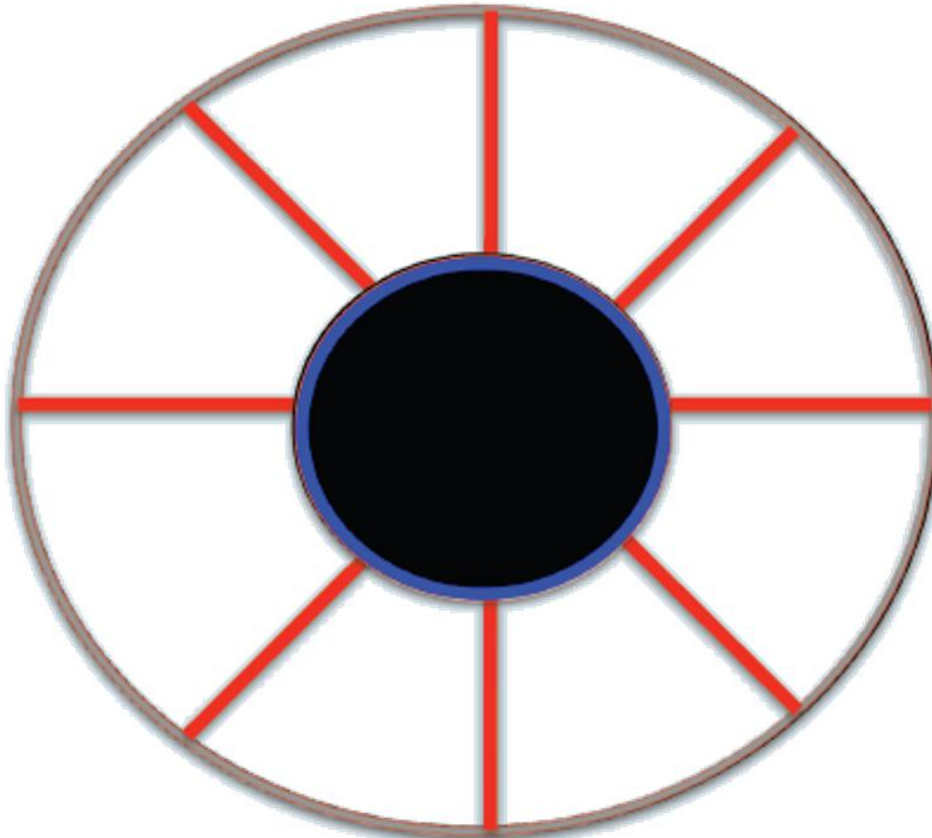
Anatomy of the Iris



These elements of the iris region may or may not be easy to visualize in any given image.

Anatomy of the Iris

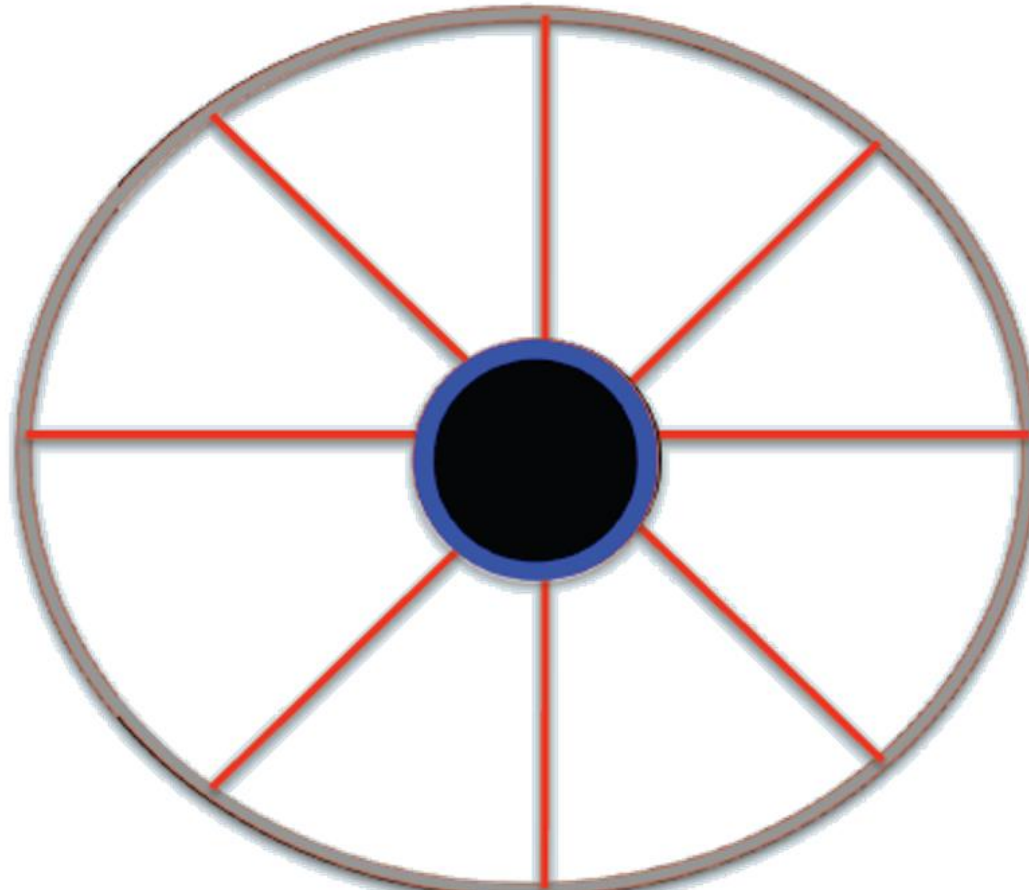
The iris has **sphincter (circular)** and **dilator (radial)** muscles that control pupil size.



- K. W. Bowyer and M. J. Burge, *Handbook of iris recognition*. Springer London, 2016.
- J. Daugman, "How iris recognition works," *IEEE Transactions on Circuits and Systems for Video Technology*, 2004

Anatomy of the Iris

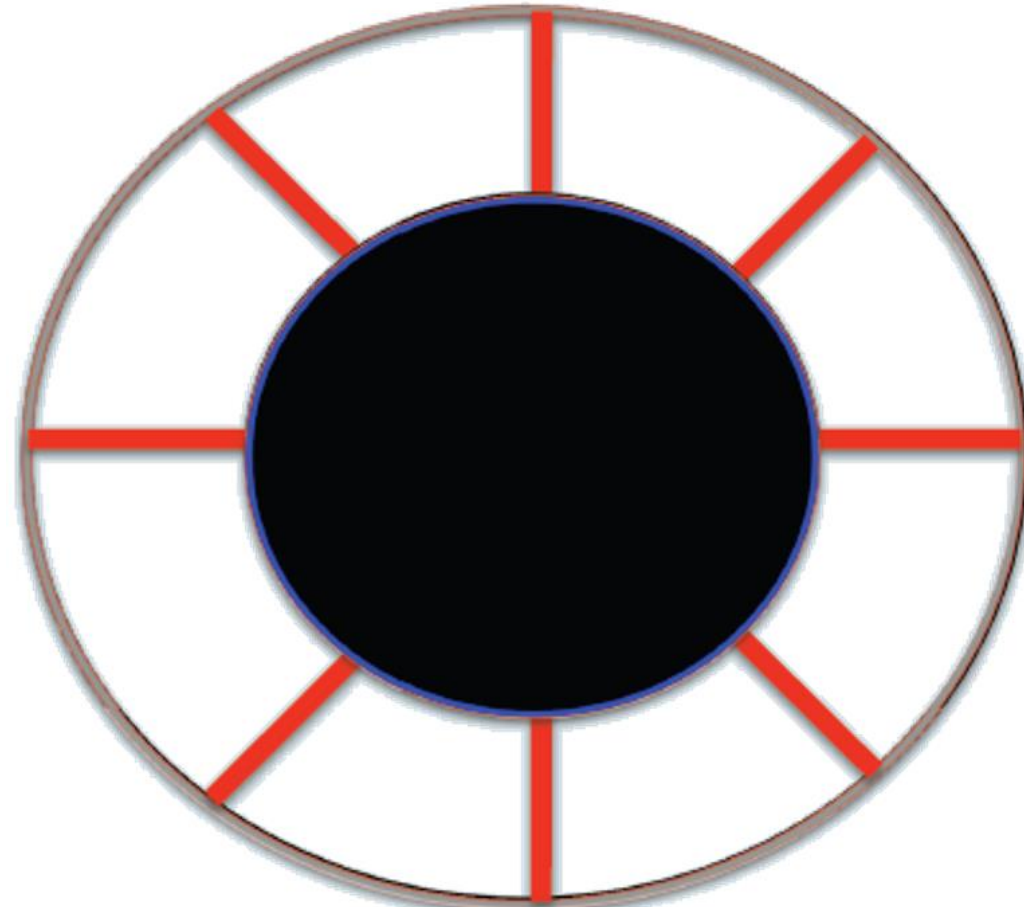
For a small pupil, the **sphincter (circular)** muscle contracts and the **dilator** relaxed (light conditions).



- K. W. Bowyer and M. J. Burge, *Handbook of iris recognition*. Springer London, 2016.
- J. Daugman, "How iris recognition works," *IEEE Transactions on Circuits and Systems for Video Technology*, 2004

Anatomy of the Iris

For a large pupil, the **dilator (radial)** muscle contracts and the **sphincter relaxes** (dark conditions).



- K. W. Bowyer and M. J. Burge, *Handbook of iris recognition*. Springer London, 2016.
- J. Daugman, "How iris recognition works," *IEEE Transactions on Circuits and Systems for Video Technology*, 2004

Anatomy of the Iris

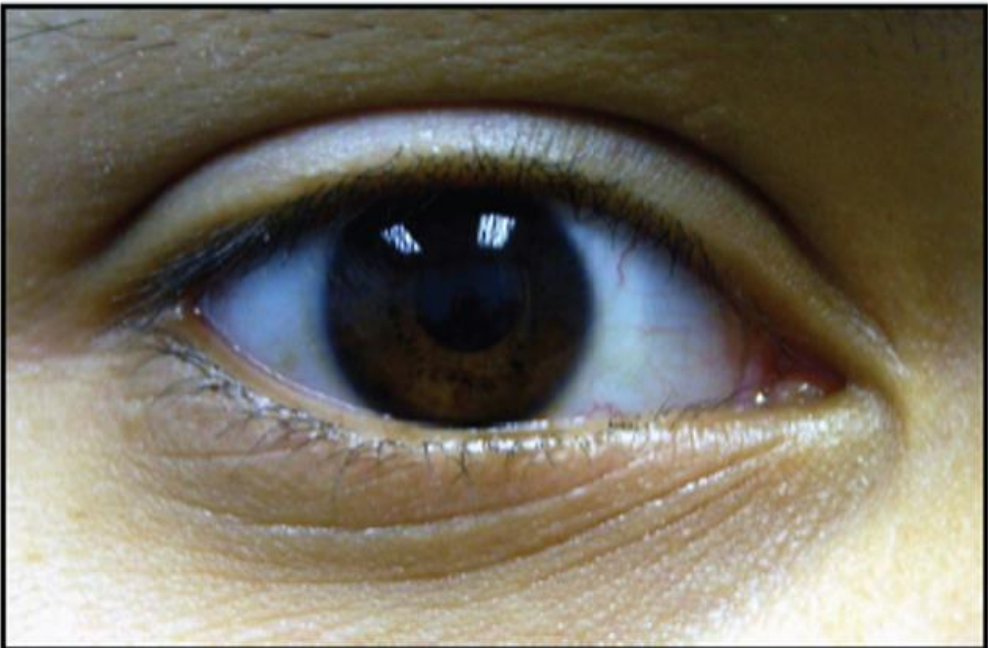
Iris acquisition? Light conditions are very important.



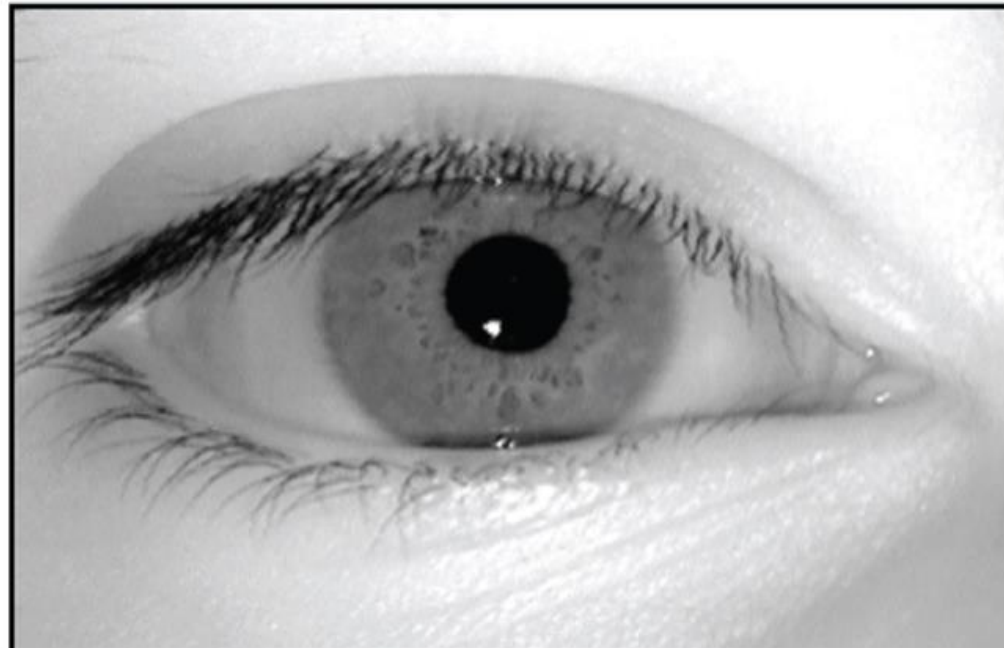
- K. W. Bowyer and M. J. Burge, *Handbook of iris recognition*. Springer London, 2016.
- J. Daugman, "How iris recognition works," *IEEE Transactions on Circuits and Systems for Video Technology*, 2004

Iris Sensors

Iris images are typically **captured using Near-InfraRed (NIR) illumination** with a wavelength ranging **between 700 nm and 900 nm**. Images acquired using such wavelengths tend to **highlight the intricate texture of the iris**, rather than its pigmentation. This helps in appropriately capturing the texture of dark-colored irises, contributing to a **better recognition performance**.



Iris in visible light



Iris in NIR

- K. W. Bowyer and M. J. Burge, *Handbook of iris recognition*. Springer London, 2016.
- J. Daugman, "How iris recognition works," *IEEE Transactions on Circuits and Systems for Video Technology*, 2004

Iris Sensors

It requires **the subject's eye to be placed within a short distance from the sensor (less than 1 m)**. Such a constraint is necessary to ensure the acquisition of high quality images that facilitate reliable recognition.



OKI IrisPass-H



LG IrisAccess



IrisID iCam T10



IrisID iCam 7000



SecuriMetrics

Automatic Iris Recognition: Architecture



Input Iris



Real or **Fake?**

Presentation Attack Detection

Detection of **attacks** from **real** irises.

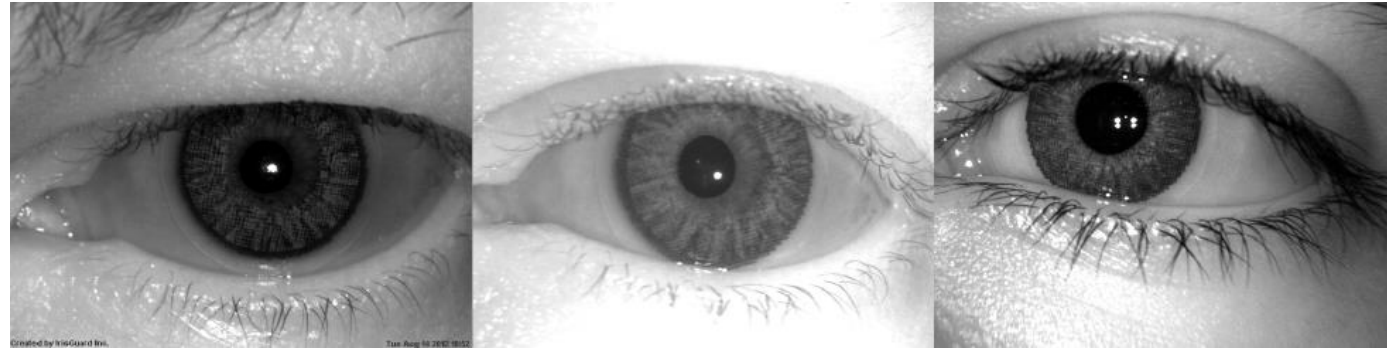


- A. Boyd, Z. Fang, A. Czajka and K.W. Bowyer, "Iris presentation attack detection: Where are we now?," *Pattern Recognition Letters*, 138, 483-489, 2020.
- D. Yadav, N. Kohli, A. Agarwal, M. Vatsa, R. Singh and A. Noore "Fusion of handcrafted and deep learning features for large-scale multiple iris presentation attack detection," in Proc. IEEE Conference on Computer Vision and Pattern Recognition Workshops, 2018.

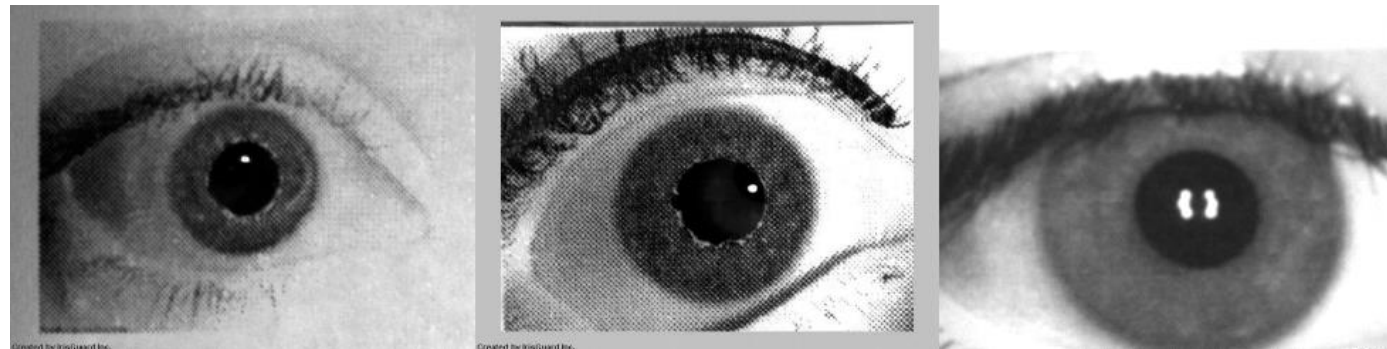
Presentation Attack Detection

Which one is **real**?

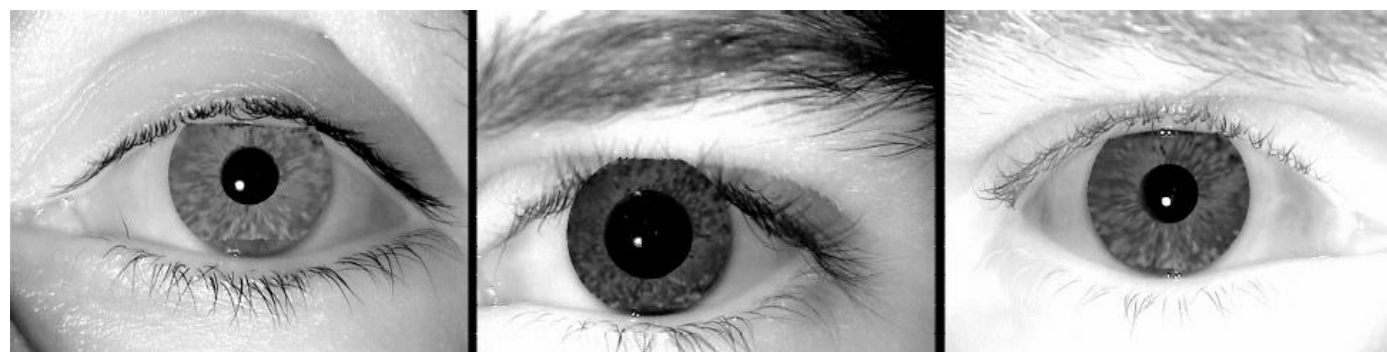
1



2



3

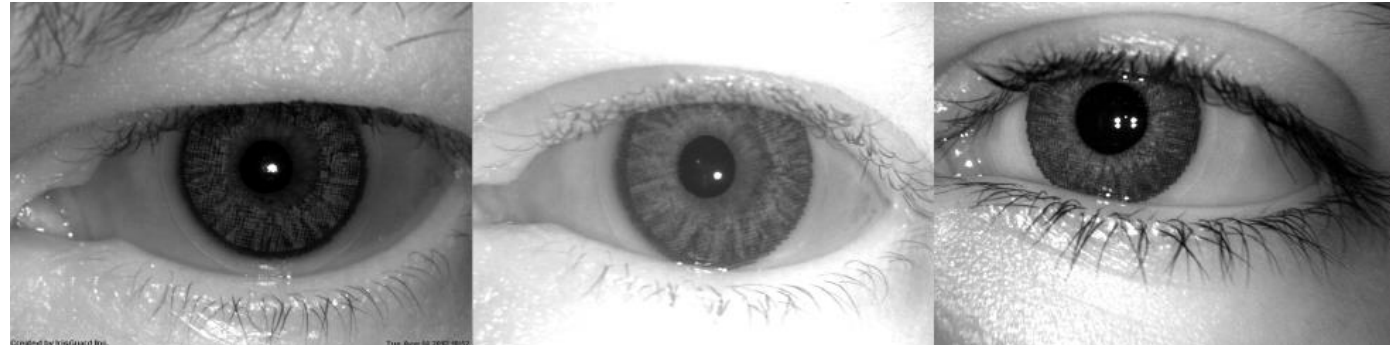


- A. Boyd, Z. Fang, A. Czajka and K.W. Bowyer, "Iris presentation attack detection: Where are we now?," *Pattern Recognition Letters*, 138, 483-489, 2020.
- D. Yadav, N. Kohli, A. Agarwal, M. Vatsa, R. Singh and A. Noore "Fusion of handcrafted and deep learning features for large-scale multiple iris presentation attack detection," in Proc. IEEE Conference on Computer Vision and Pattern Recognition Workshops, 2018.

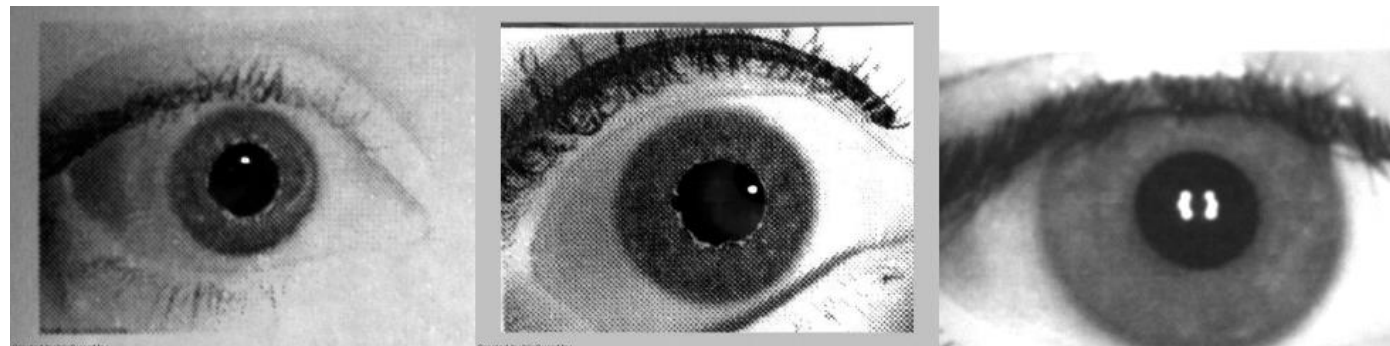
Presentation Attack Detection

Which one is **real**?

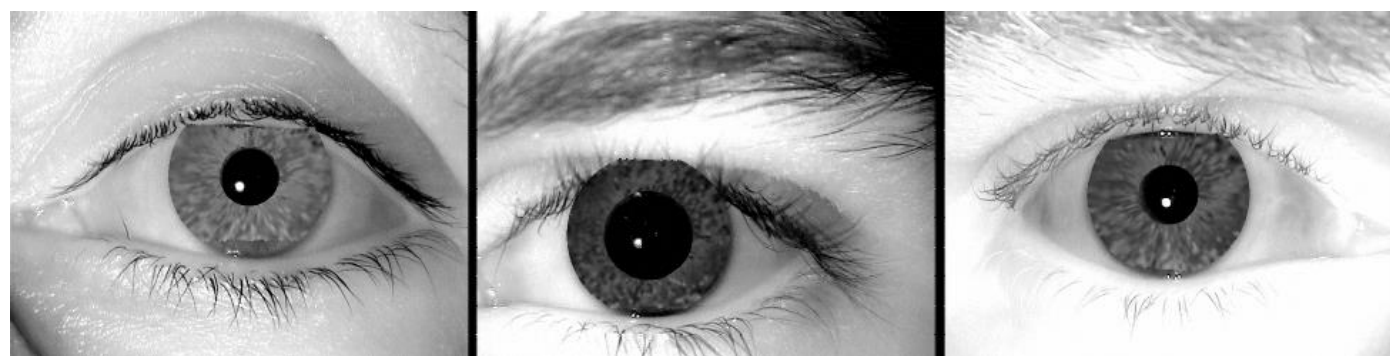
Fake: Textured Contact Lenses



Fake: Printed Iris Images



Fake: Synthetic Iris Images

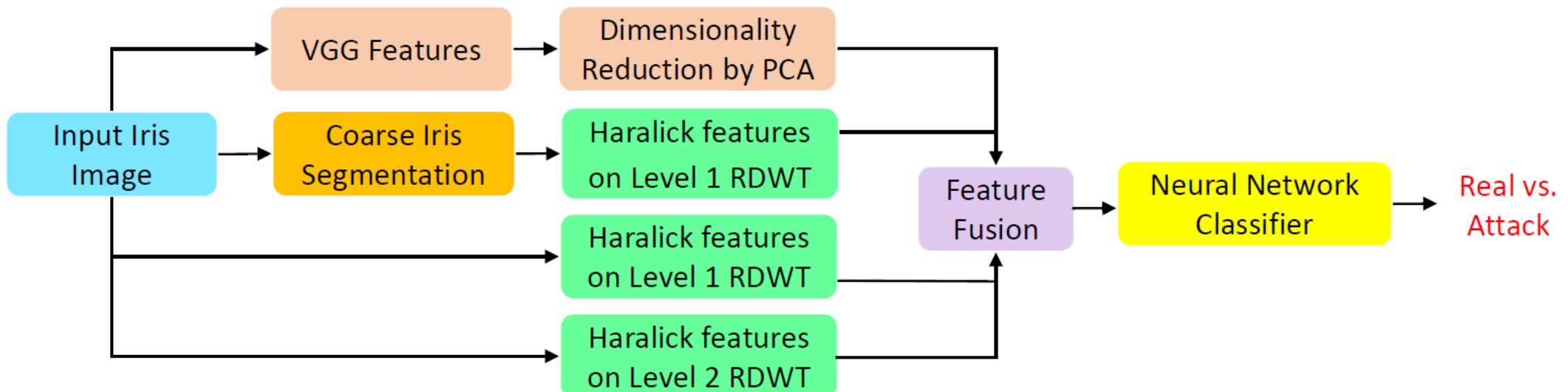


- A. Boyd, Z. Fang, A. Czajka and K.W. Bowyer, "Iris presentation attack detection: Where are we now?," *Pattern Recognition Letters*, 138, 483-489, 2020.
- D. Yadav, N. Kohli, A. Agarwal, M. Vatsa, R. Singh and A. Noore "Fusion of handcrafted and deep learning features for large-scale multiple iris presentation attack detection," in Proc. IEEE Conference on Computer Vision and Pattern Recognition Workshops, 2018.

Presentation Attack Detection

Fusion of handcrafted and deep learning features:

- **Handcrafted:** local and global Haralick texture features in Redundant Discrete Wavelet Transform.
- **Deep Learning:** VGG16 architecture pre-trained with ImageNet database.
- **Fusion:** concatenation of handcrafted and deep learning features.
- **Classifier:** three-layer Multilayer Perceptron (MLP).



Presentation Attack Detection

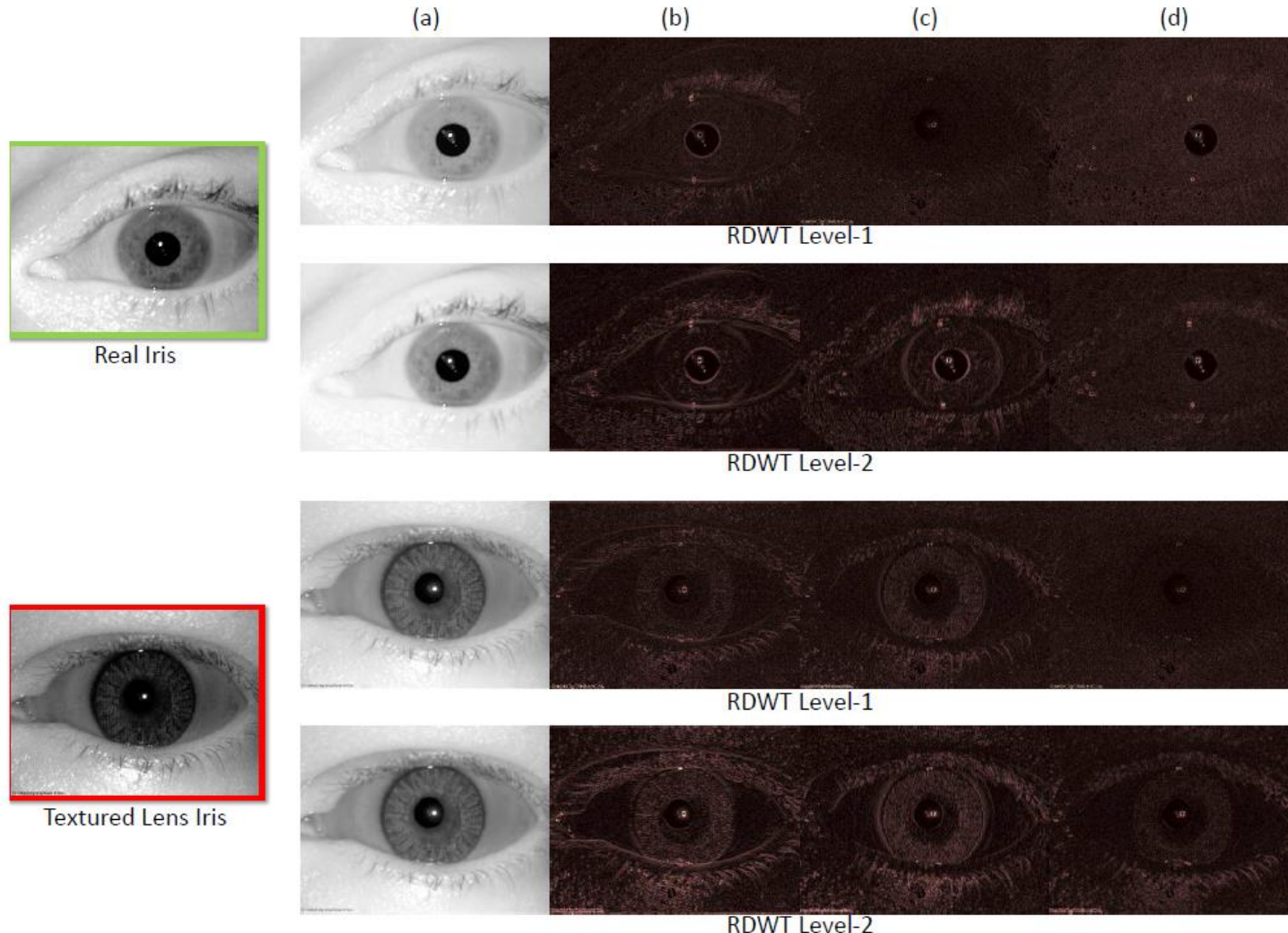


Figure 3. RDWT decomposition of a real iris image and textured contact lens iris image: (a) approximation subband, (b) horizontal subband, (c) vertical subband, and (d) diagonal subband.

- D. Yadav, N. Kohli, A. Agarwal, M. Vatsa, R. Singh and A. Noore "Fusion of handcrafted and deep learning features for large-scale multiple iris presentation attack detection," in Proc. IEEE Conference on Computer Vision and Pattern Recognition Workshops, 2018.

Presentation Attack Detection

Experimental results:

Table 1. Characteristics of the Combined Iris Database and its constituent databases.

Database	No. of Iris Images	Type(s) of Iris Images
LivDet2013 (Warsaw Subset) [7]	1,667	Print and Real
Combined Spoofing Database [14]	21,525	Real, Print, Textured Contact Lens, and Synthetic Iris
NDCLD-2013 [4]	4,200 (LG4000) and 900 (AD100)	Real and Textured Contact Lens
NDCLD-2015 [9]	7,300	Real and Textured Contact Lens
ND-Iris-0405	64,980	Real
ND-CrossSensor-Iris-2013	117,106 (LG2200) & 29,845 (LG4000)	Real
ND-TimeLapseIris-2012	6,796	Real
CASIA-Iris-Thousand	20,000	Real
Combined Iris Database	274,319	Real, Print, Textured Contact Lens, and Synthetic Iris

Presentation Attack Detection

Experimental results:

Table 3. Iris presentation attack detection performance (%) of the proposed MHVF and existing algorithms on the Combined Iris database.

Algorithm	Total Error	APCER	BPCER
LBP [6]	22.94	80.00	20.00
WLBP [10]	52.75	48.18	53.00
DESIST [14]	4.13	77.48	0.20
MH	3.36	59.96	0.32
VGG [19]	1.53	21.83	0.44
Proposed MHVF	1.01	18.58	0.07

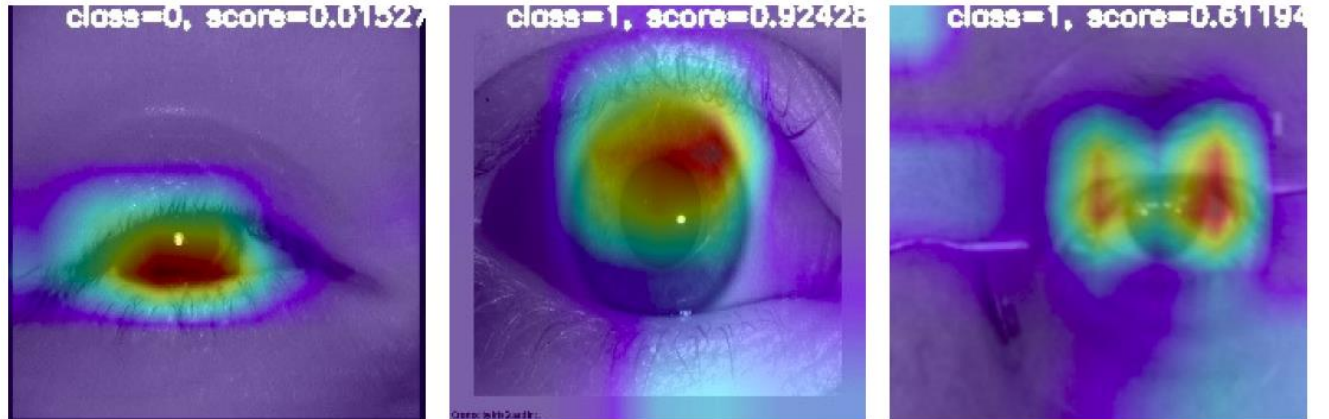
Errors of 18.58% in detecting presentation attacks!!!

Presentation Attack Detection

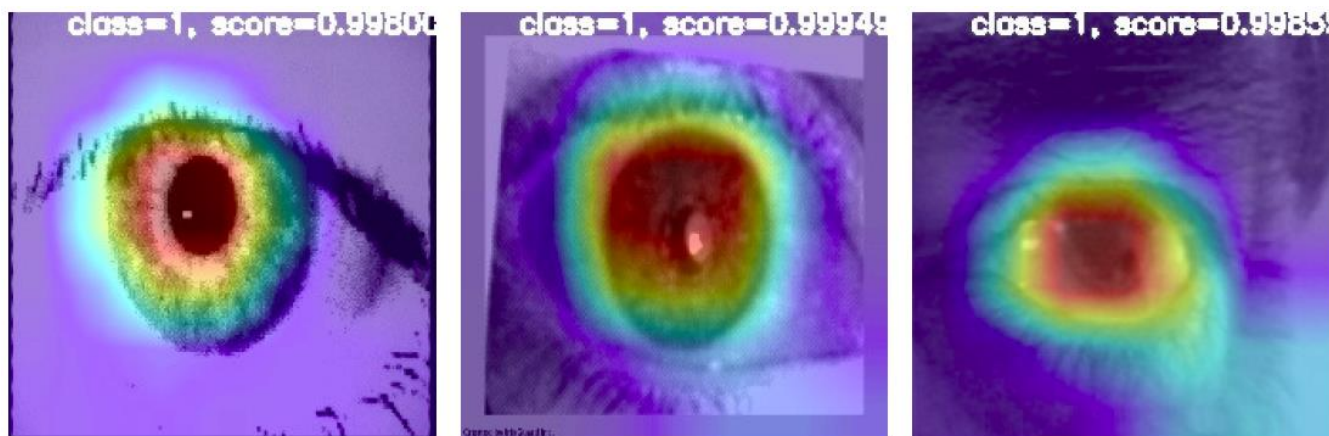
Similar results in the latest publications:

- Deep learning architectures (Inception V3, ResNet50, and MobileNetV2) pre-trained with ImageNet.
- Transfer learning techniques: convolutional layers are frozen. Last fully-connected layer is trained.

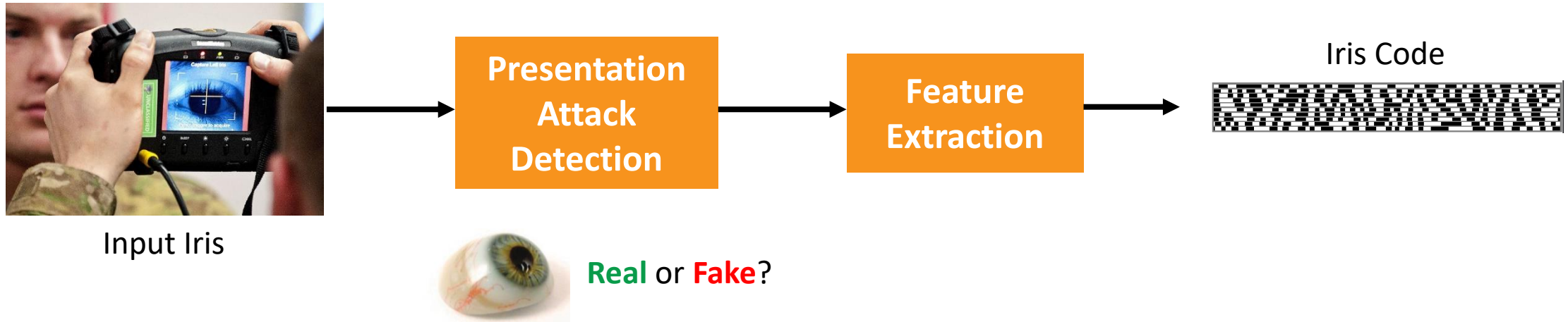
Errors: Real



Errors: Fake

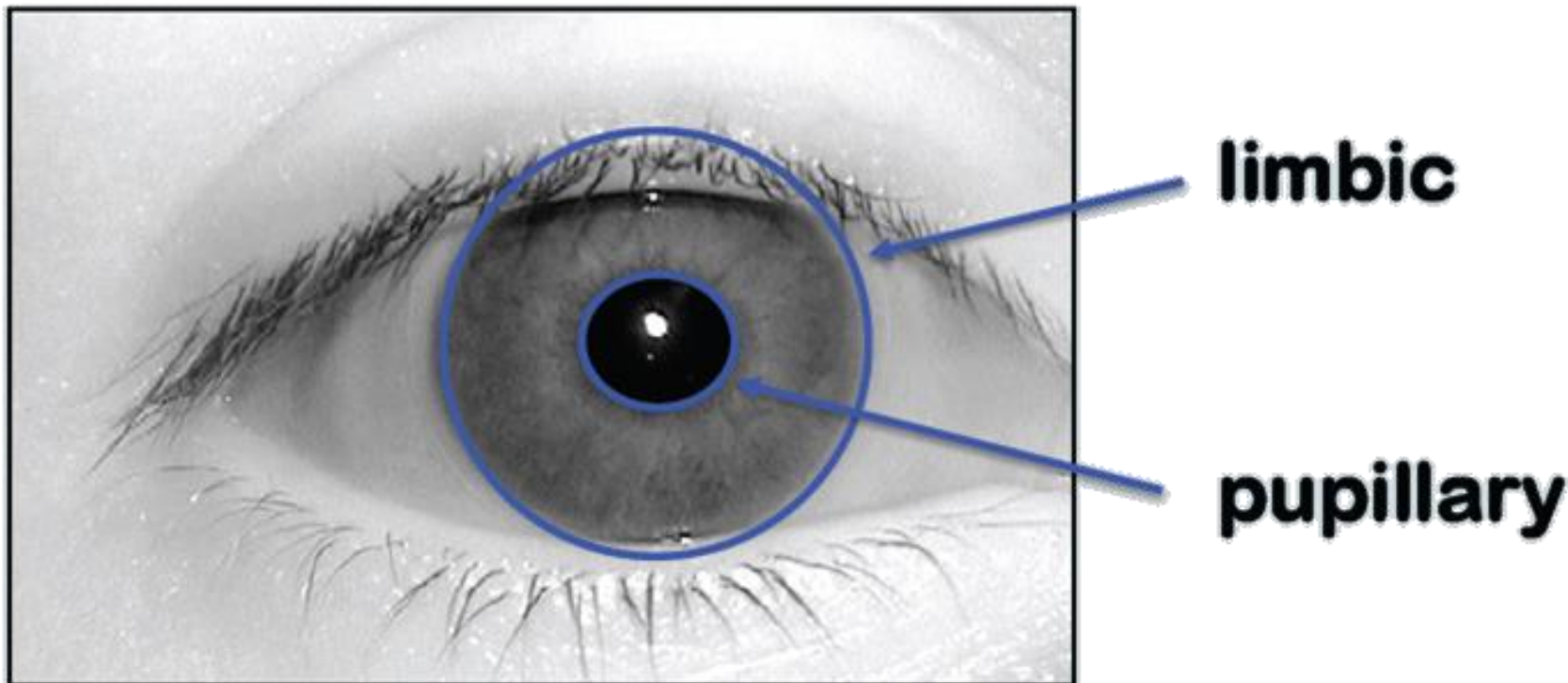


Automatic Iris Recognition: Architecture



Segmentation

The main step is to find the **pupillary** (inner) and **limbic** (outer) boundaries.



Segmentation

Historically, the iris has been found with Daugman's integro-differential operator or circular edge detector. The task is to find the center coordinates and the radius of the iris and the pupil.

$$\max_{(r, x_0, y_0)} \left| G_\sigma(r) * \frac{\partial}{\partial r} \oint_{r, x_0, y_0} \frac{I(x, y)}{2\pi r} ds \right|$$

$I(x, y)$ is the intensity of the pixel at coordinates (x, y) in the image of an iris.

r denotes the radius of various circular regions with the center coordinates at (x_0, y_0) .

σ is the standard deviation of the Gaussian distribution.

$G_\sigma(r)$ denotes a Gaussian filter of scale sigma (σ).

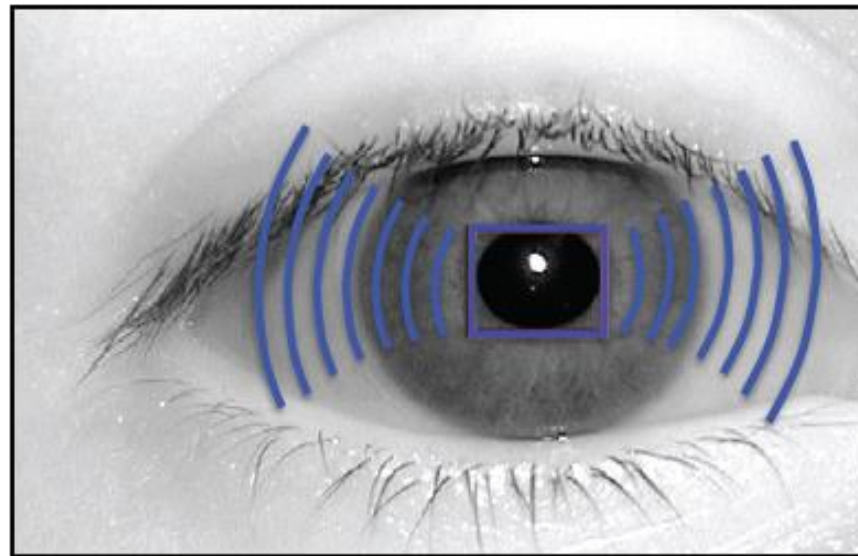
(x_0, y_0) is the assumed centre coordinates of the iris.

s is the contour of the circle given by the parameters (r, x_0, y_0) .

The operator searches over the image domain (x, y) for the maximum in the blurred (due to the Gaussian filter) partial derivative with respect to increasing radius r , of the normalized contour integral of $I(x, y)$ along a circular arc ds of radius r and center (x_0, y_0) .

Segmentation

The bounding box of the **largest dark region** might be a range to search for x_0 , y_0 with r in a feasible range:

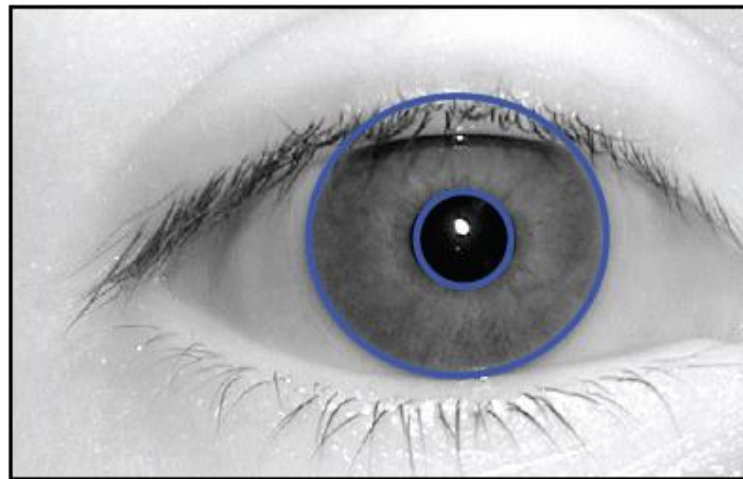


Non-circular pupillary and limbic boundaries have been handled by:

- Fitting ellipses.
- Fitting circles and adjusting using active contours.
- Using “balloon” active contours.

Segmentation

The inner and outer boundaries are used to “unwrap” the iris region to a rectangle.

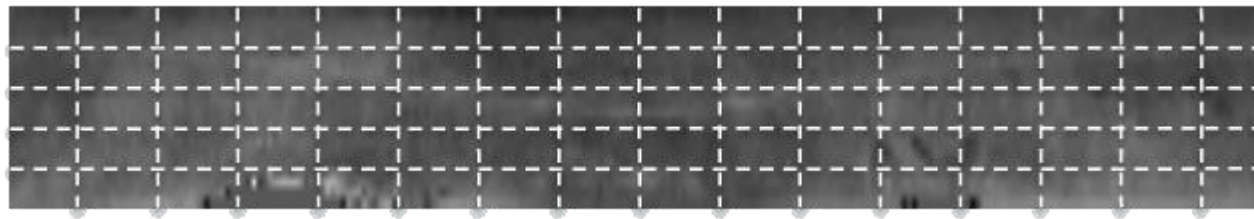


All iris regions in all images are mapped to the same size rectangular version.

This is the “rubber sheet” model, linearly stretching or compressing the imaged iris to a standard size frame.

Segmentation

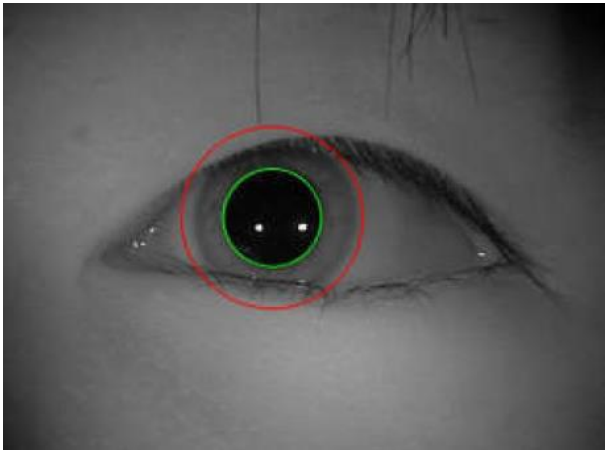
Texture filters can then be applied at a fixed grid on the rectangle to generate the same size iris code for any image.



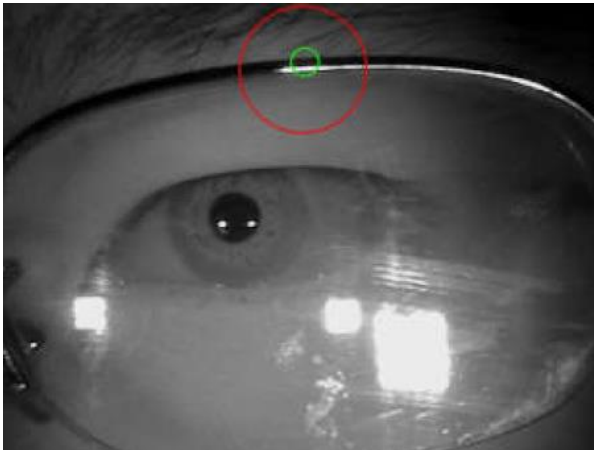
The rectangular image also has a binary mask that tells where the iris region was occluded / what iris code bits not to use.



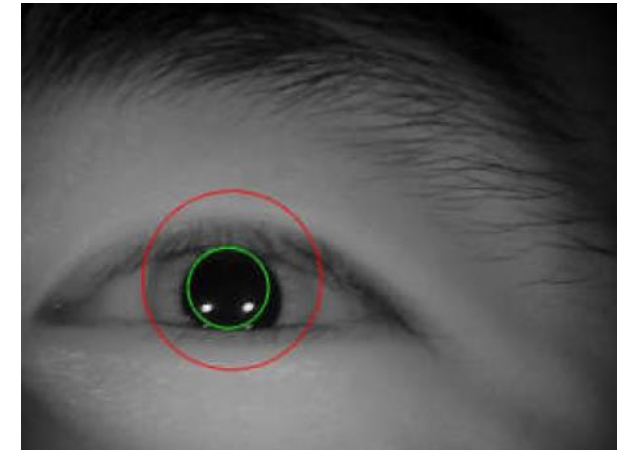
Segmentation Challenges



Unclear Boundaries



Eyeglasses

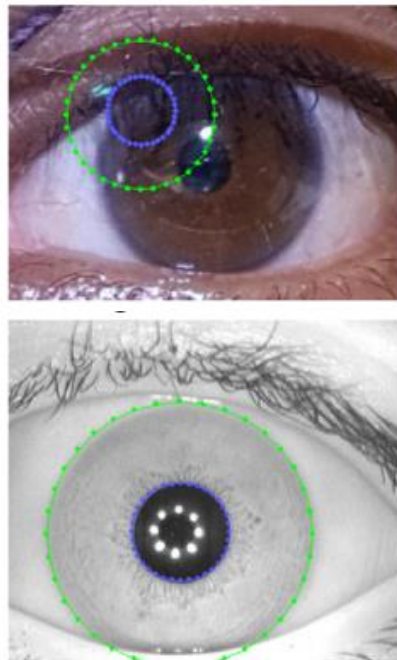


Occlusion

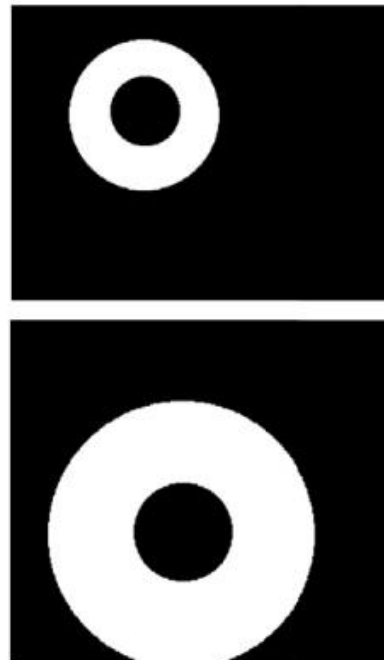
Segmentation

CNN-based iris segmentation have been proven to be superior to traditional iris segmentation techniques.

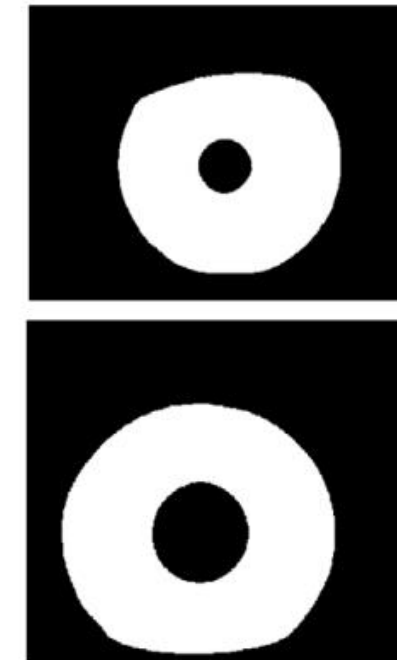
Daugman
Segmentation



Daugman
Mask



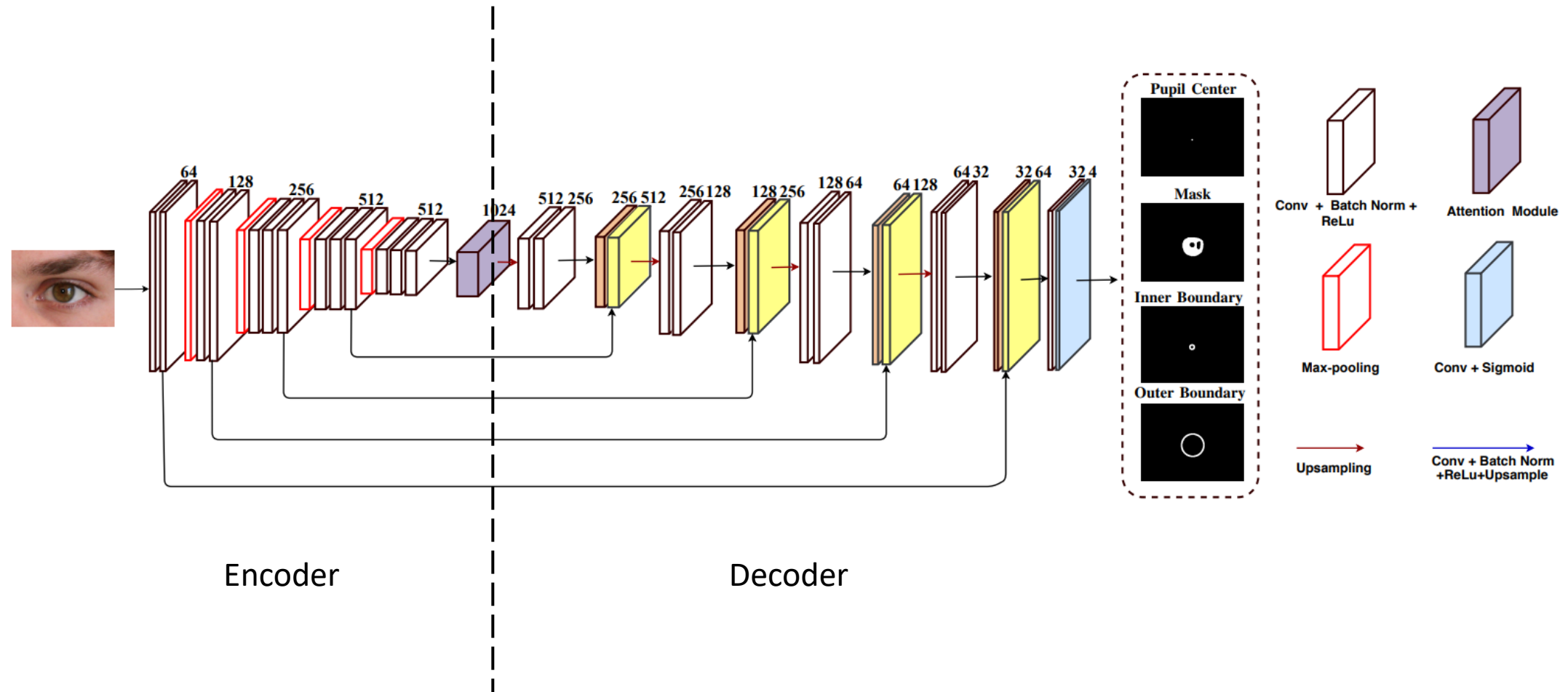
CNN
Mask



- H. Hofbauer, E. Jalilian and A. Uhl, "Exploiting superior CNN-based iris segmentation for better recognition accuracy," *Pattern Recognition Letters*, 120, 17-23, 2019.
- N. Liu, H. Li, M. Zhang, J. Liu, Z. Sun and T. Tan, "Accurate iris segmentation in non-cooperative environments using fully convolutional networks," in Proc. International Conference on Biometrics, 2016.
- E. Jalilian, A. Uhl, B. Bhanu, A. Kumar, "Iris Segmentation Using Fully Convolutional Encoder–Decoder Networks", *Deep Learning for Biometrics*, Springer, 2017.

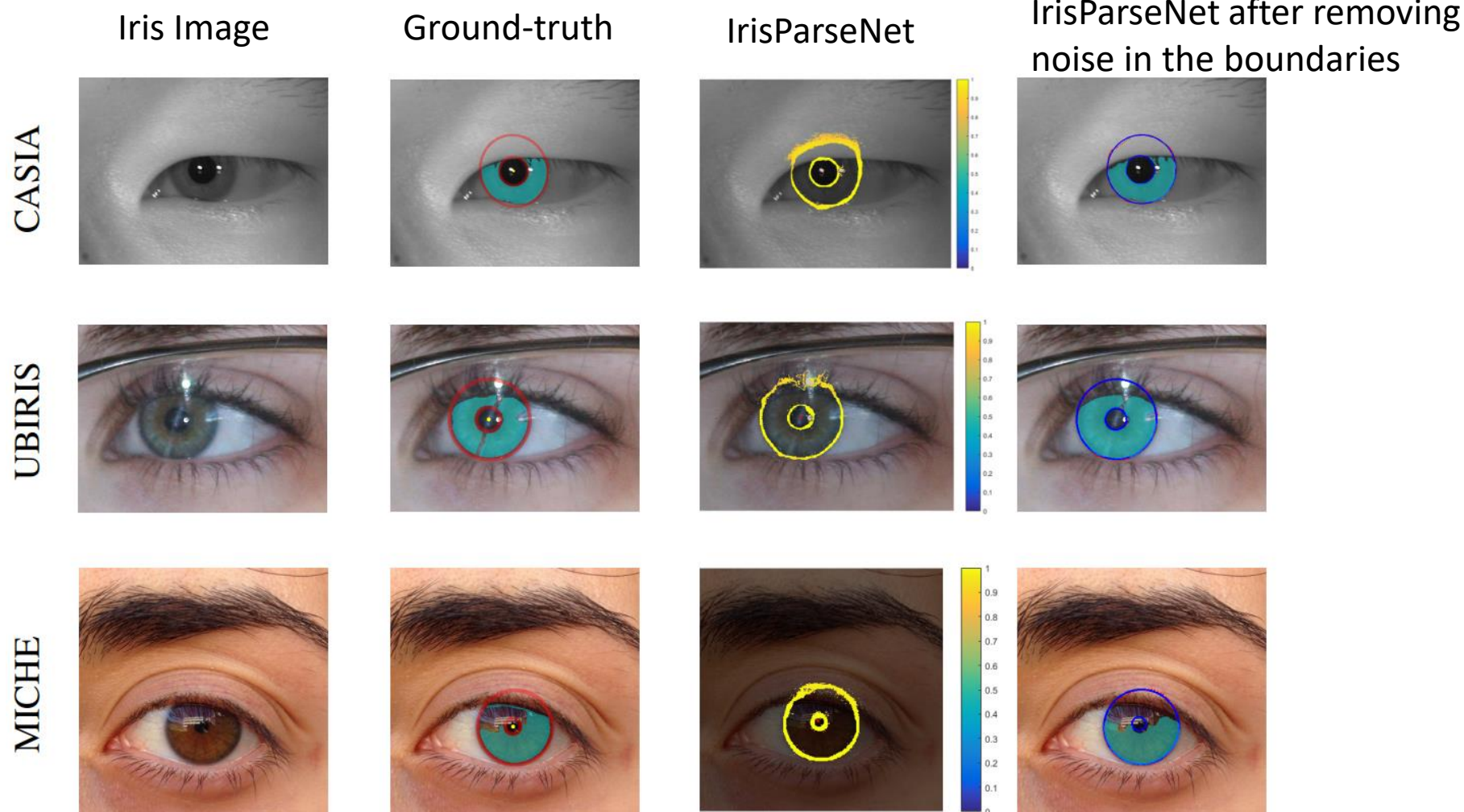
Segmentation

IrisParseNet - Deep multi-task learning framework: iris segmentation and localization at the same time.



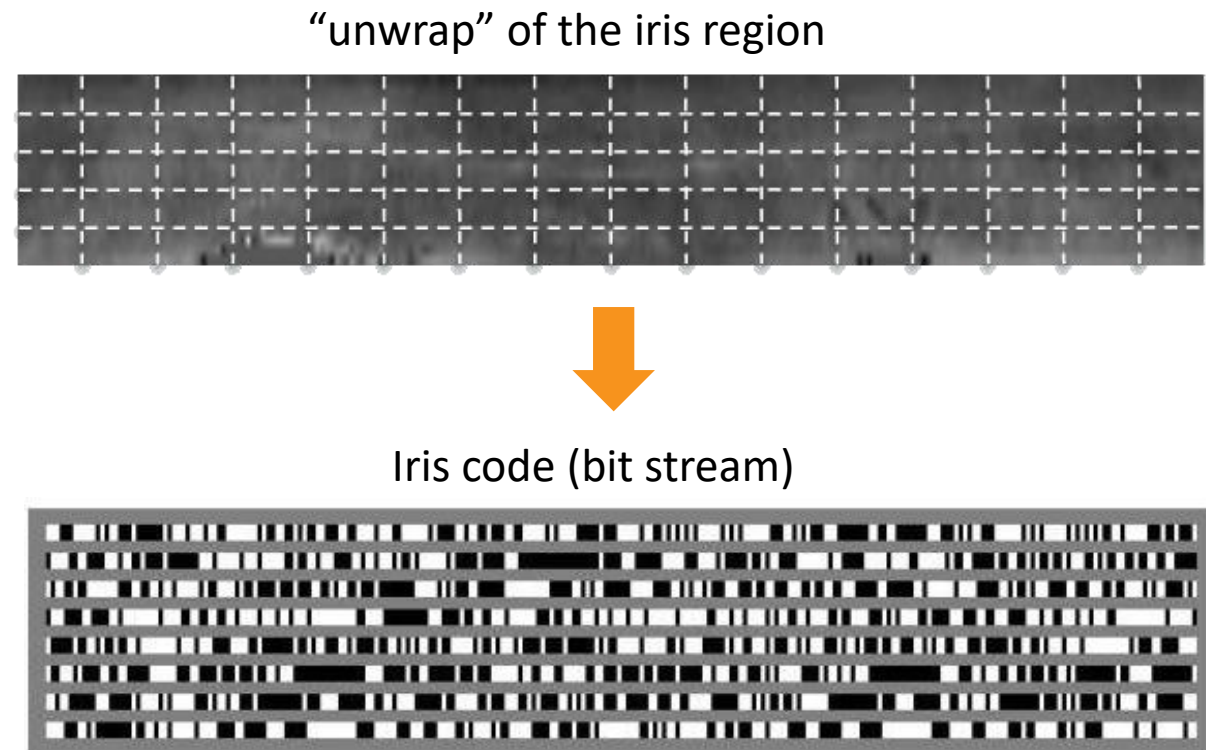
Segmentation

IrisParseNet - Deep multi-task learning framework: iris segmentation and localization at the same time.



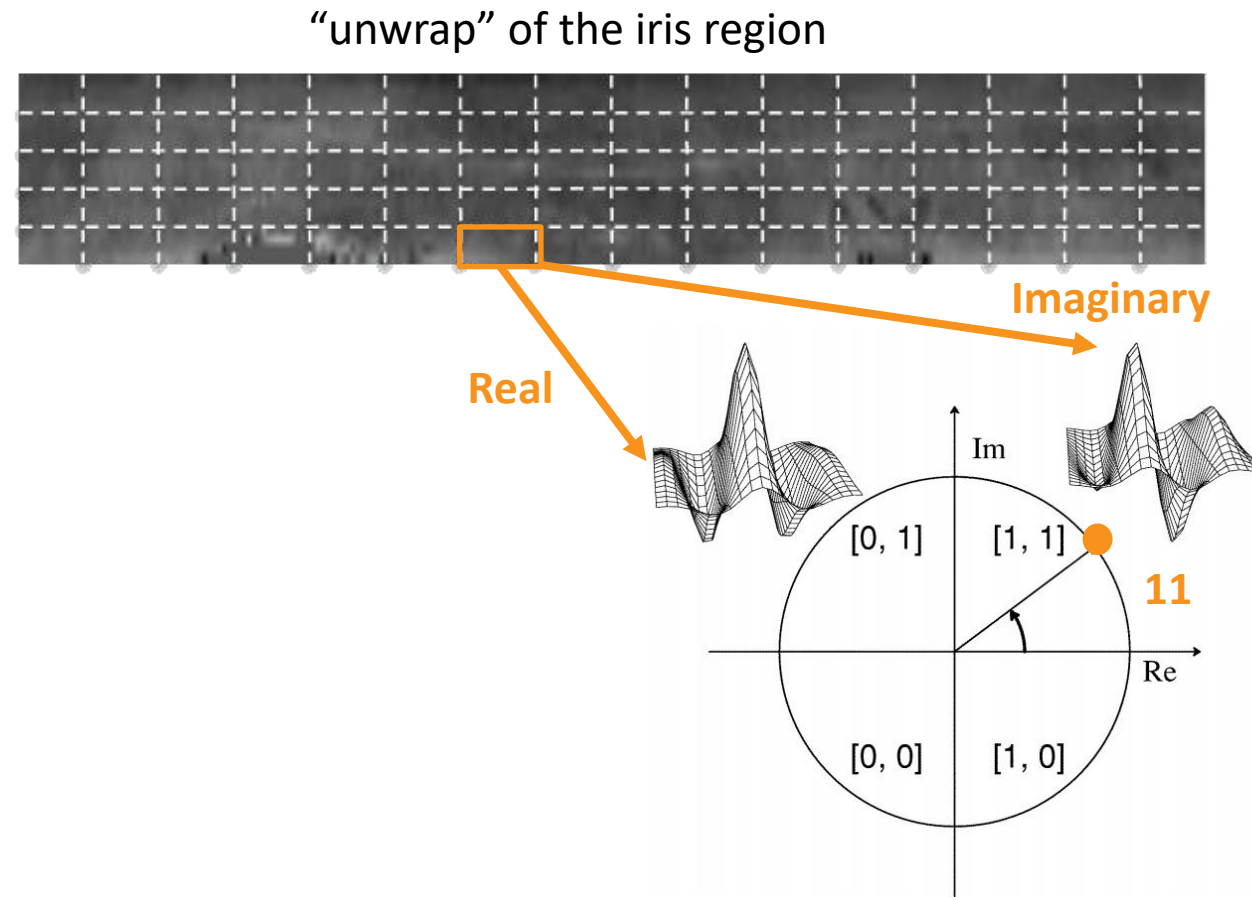
Feature Extraction: Iris Code

The **bit stream (iris code)** is the result of demodulation with complex-valued **two-dimensional (2D) Gabor filter** to encode **the phase sequence** of the iris pattern.



Feature Extraction: Iris Code

Applying the 2D Gabor filter to each patch location of the iris image results in a point in the complex plane. The phase of the complex value makes two bits in the iris code (phase-quadrant demodulation code).

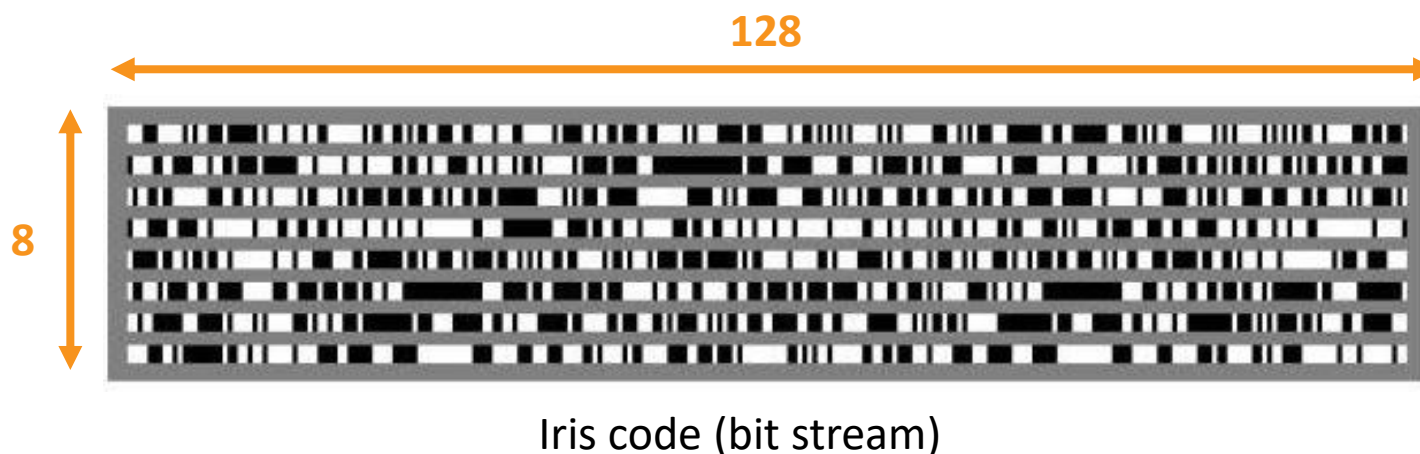


Feature Extraction: Iris Code

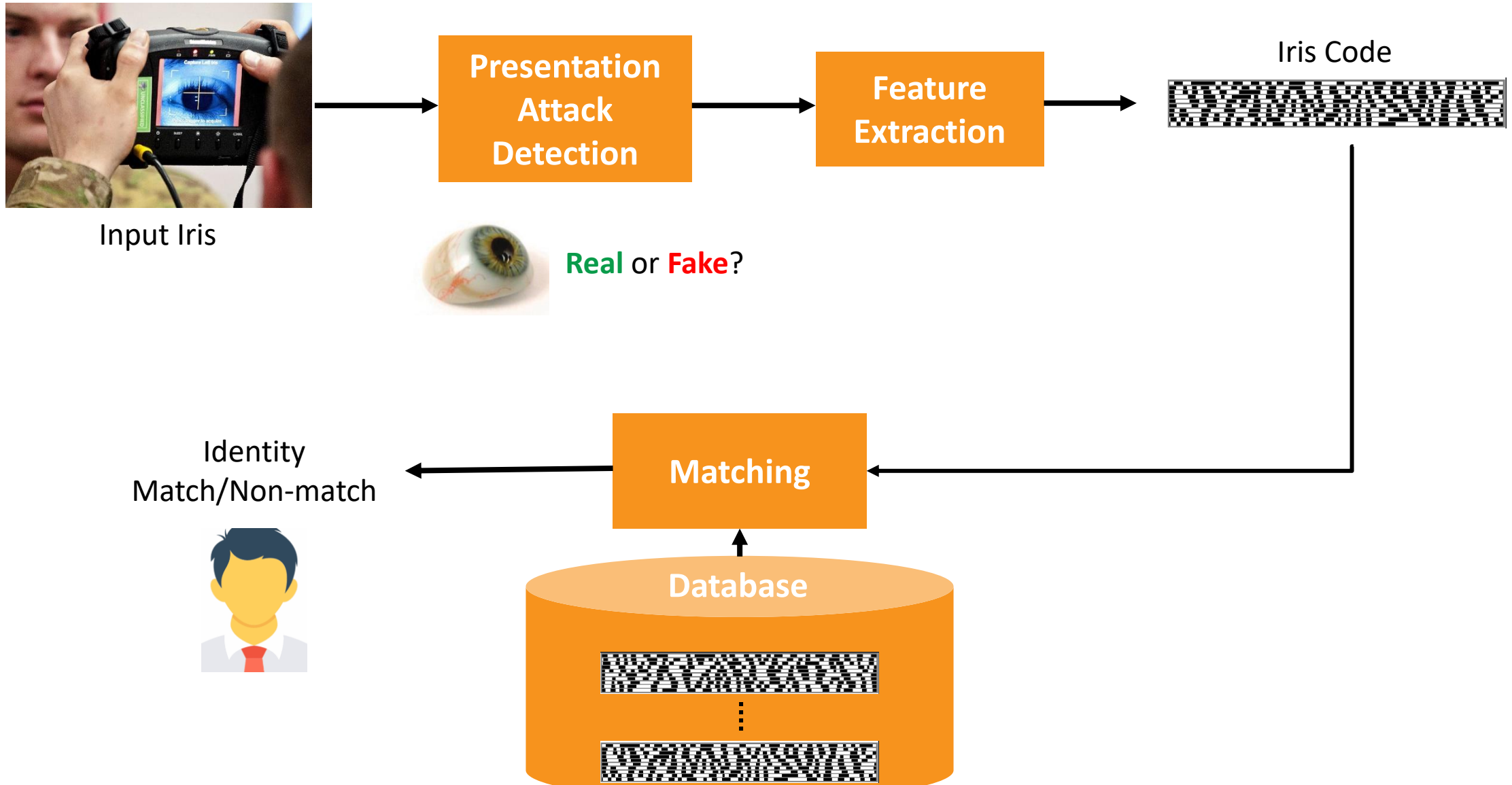
Applying the 2D Gabor filter to each patch location of the iris image results in a point in the complex plane. The phase of the complex value makes two bits in the iris code (phase-quadrant demodulation code).

The standard commercial iris code is 2,048 bits (plus 2,048-bit mask).

- 2,048 bits / 2 bits per path = 1,024 path samples are considered from the iris image.
- 1,024 = 8 rows x 128 columns is a plausible path configuration.



Automatic Iris Recognition: Architecture

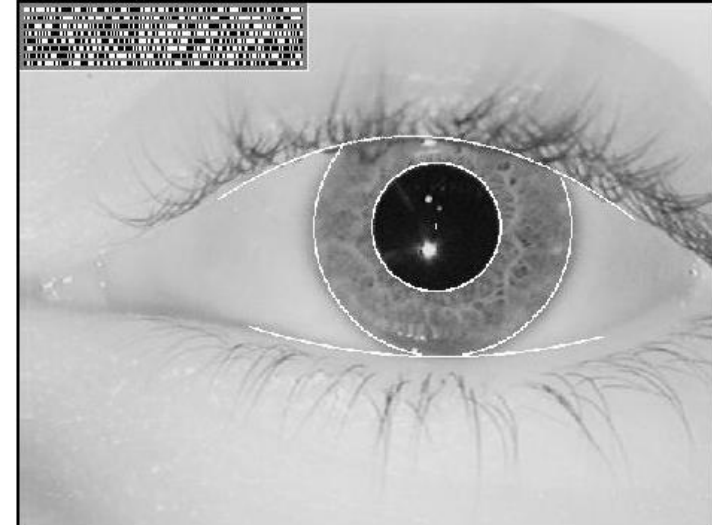
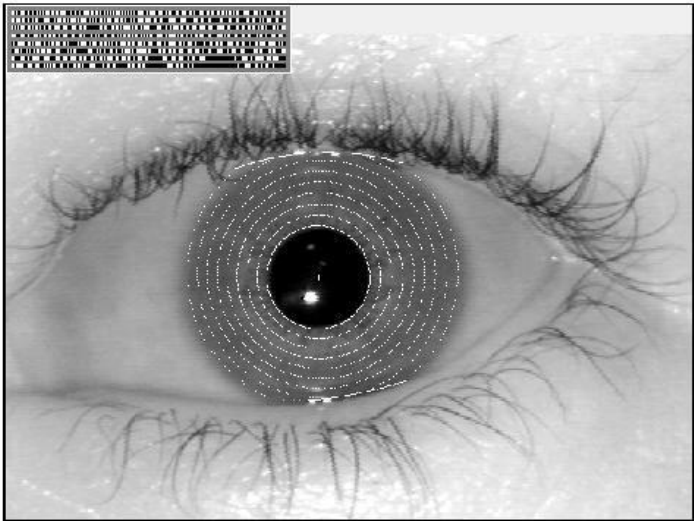


Matching

The metric for comparing iris codes is the **fractional Hamming distance (FHD)**.

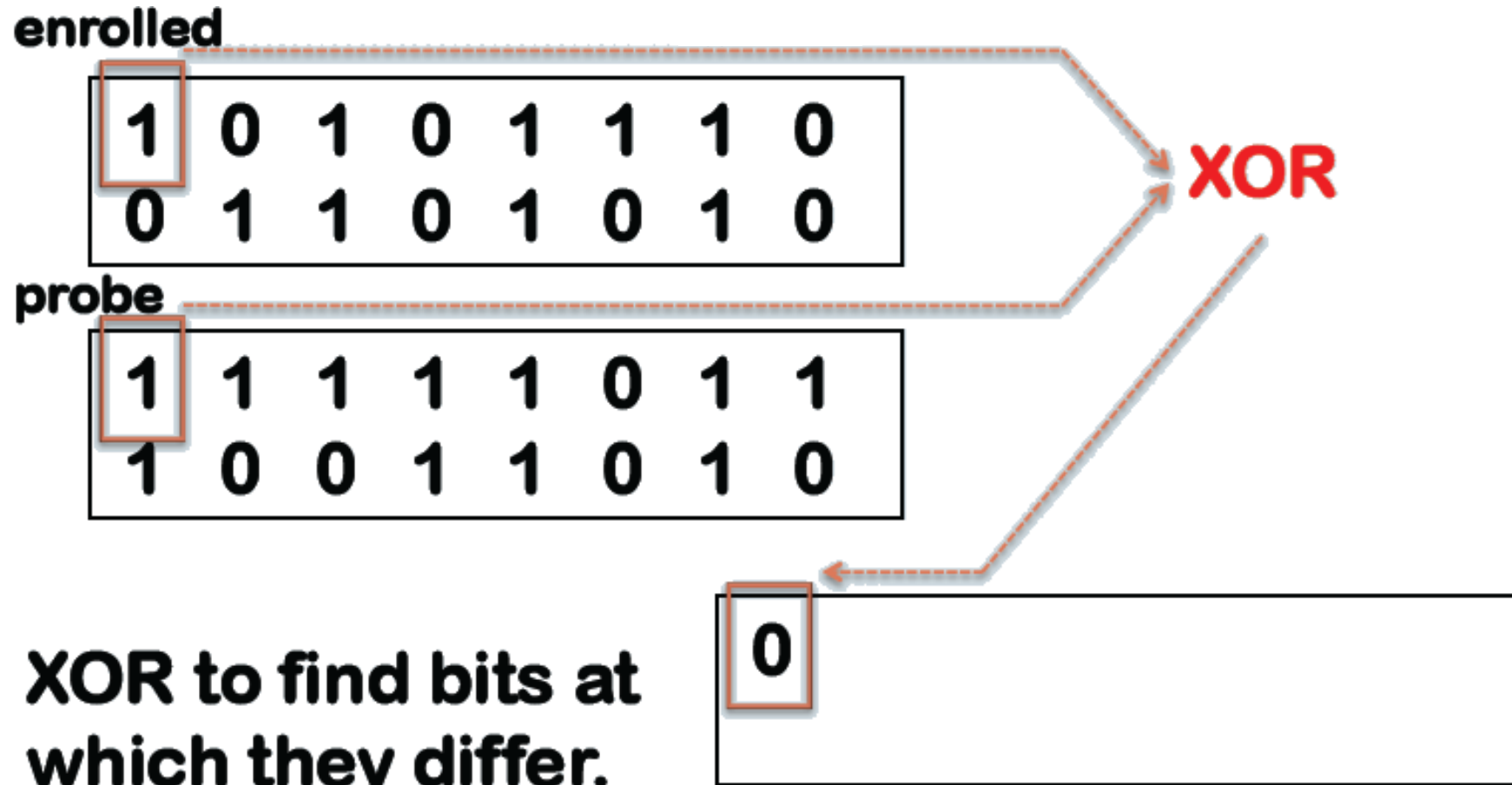
It is a difference metrics:

- min value of **0.0** means no difference.
- max of **1.0** means totally different.
- **0.5** value means random agreement.



Matching

The metric for comparing iris codes is the [fractional Hamming distance \(FHD\)](#).



Matching

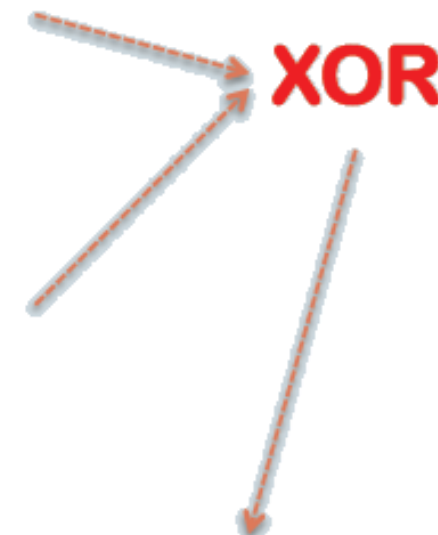
The metric for comparing iris codes is the [fractional Hamming distance \(FHD\)](#).

enrolled

1	0	1	0	1	1	1	0
0	1	1	0	1	0	1	0

probe

1	1	1	0	0	0	1	1
1	0	0	1	1	0	1	0



**FHD is the fraction
of bits that differ;
here, FHD = 0.5**

0	1	0	0	1	1	0	1
1	1	1	1	0	0	0	0

Matching

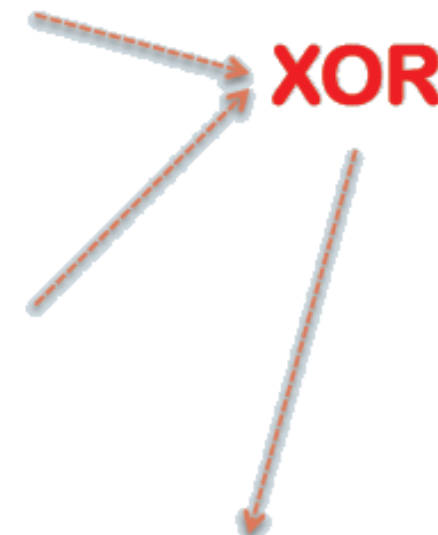
The metric for comparing iris codes is the **fractional Hamming distance (FHD)**.

enrolled

1	0	1	0	1	1	1	0
0	1	1	0	1	0	1	0

probe

1	1	1	0	0	0	1	1
1	0	0	1	1	0	1	0



**FHD is the fraction
of bits that differ;
here, FHD = 0.5**

0	1	0	0	1	1	0	1
1	1	1	1	0	0	0	0

Matching

Using other **features** and **machine learning** techniques.

#	<i>Authors, Year</i>	<i>Dataset</i>	<i>Peri ocular</i>	<i>Features</i>	<i>Rec. %</i>	<i>ML Approach</i>
1	Abiyev and Altunkaya, 2008	CASIA-IrisV1	N	Intensity image	99.25	Neural network featuring gradient based learning algorithm with adaptive learning rate
2	AL-Allaf et al, 2013	CASIA-IrisV1	N	Partitioned intensity image	98.9	Feedforward Back Propagation Neural Network (FBPNN)
3	Ali and Salami, 2008	CASIA-IrisV1	N	Gabor wavelet	100 ?	Support Vector Machine (SVM)
4	Baqar et al. 2011	MMU Iris Database	N	Dual boundary contour vector	99	Dual boundary detection via robust variable learning rate Multilayer Feedforward Neural Network(MFNN)
5	Chen and Chu, 2005	CASIA	N	Sobel and vertical projections	EER =3,32 %	Wavelet Neural Network and Probabilistic Neural Network
6	Chowan et al, 2011	CASIA-IrisV1	N	Singular Value Decomposition (SVD)	94	Modified Fuzzy HyperSphere Neural Network with different distance measures (MFHSNN)
7	Chowan and Shinde, 2011	CASIA-IrisV1	N	SVD	95.68	Fuzzy Min-Max Neural Network
8	Chu and Chen, 2005	CASIA-IrisV1	N	LPCC / Linear Discriminant Analysis (LDA)	99.14	Particle Swarm Optimization (PSO) + Probabilistic Neural Network (PNN)
9	Dias et al, 2010	CASIA-IrisV1	N	Intensity image	94.24	Back Propagation Neural Network (BPNN), various back propagation algorithms

Matching

Using other **features** and **machine learning techniques**.

19	Melin et al, 2012	CASIA-IrisV3	N	Wavelet transform	99.76	ANN + Fuzzy Integrator + Genetic Algorithm
20	Moinuddin et al, 2004	Daugman's iris dataset	N	1D iris contour	97	Multilayer Feedforward Neural Network (MFNN) and Radial Basis Function Neural Network (RBFNN)
21	Nie et al, 2014	UBIPr	Y		50.1	Unsupervised Convolutional Restricted Boltzmann Machine (RBM) Feature Learning
22	X Pillai et al, 2013	Notre Dame (ND)	N	Daugman's iris code	87.82	Kernel-learning framework for cross-sensor adaptation
23	Raghavi et al, 2011	Proprietary	N	Haar wavelet	99.25	Fuzzy Neural Network (FNN) algorithm
24	Rai and Yadav, 2014	CASIA-IrisV1 CHECK	N	Haar wavelet decomposition / 1D Log Gabor wavelet	99.91 99.88	Support Vector Machines (SVM) and Hamming distance
25	Raja and Rajagopalan, 2013	N/A	N	?	98.48	Artificial Neural Network (ANN) + Genetic algorithm (GA)
26	Roy et Bhattacharya , 2005	CASIA_IrisV1	N	Gabor wavelet	97.34	Support vector Machine (SVM) with different kernel types
27	Roy et Bhattacharya , 2007	ICE WVU	N	2D Gabor wavelets	97.7 95.6	Multi-Objective Genetic Algorithm (MOGA) and asymmetrical Support Vector Machine (SVM)
28	Saminathan et al, 2015	CASIA-IrisV3-Interval	N	Intensity image	98.5	Least square method of quadratic kernel Support Vector machine (SVM)
29	Sarhan, 2009	CASIA-IrisV2	N	2D Discrete Cosine Transform (DCT)	96	Artificial Neural Networks (ANN)

Performance of Iris Recognition

Table 2
Reported recognition results

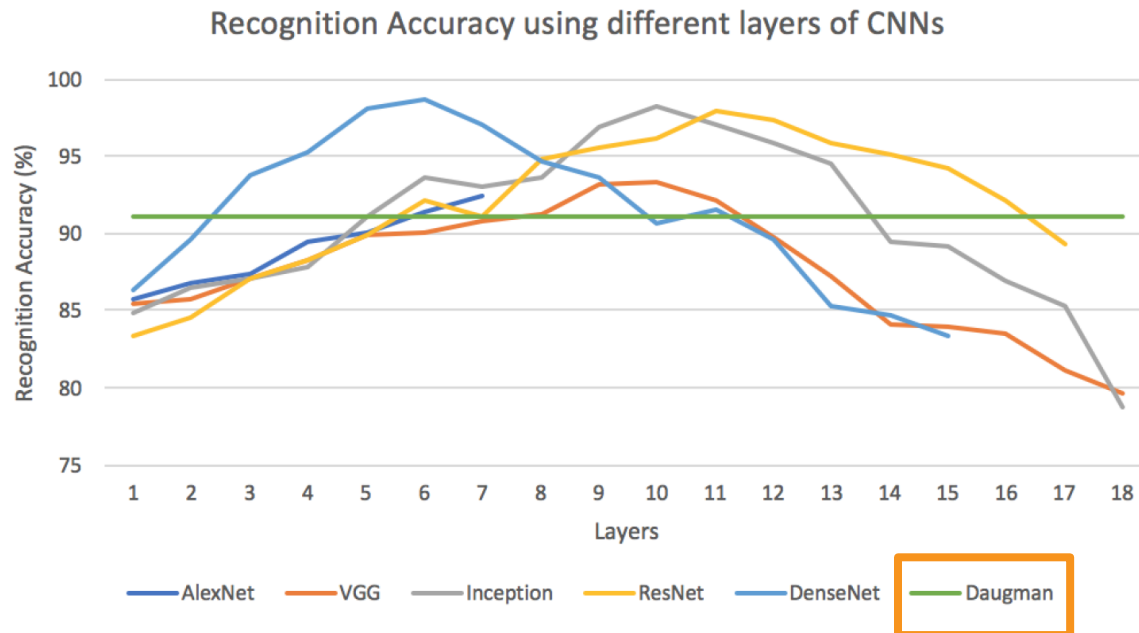
First author, year	Size of database	Results
Alim, 2004 [4]	Not given	96.17%
Jang, 2004 [70]	1694 images including 160 w/glasses and 11 w/contact lenses	99.1%
Krichen, 2004 [80]	700 visible-light images	FAR/FRR: 0%/ 0.57%
Liu, 2005 [87]	4249 images	97.08%
Ma, 2002 [94]	1088 images	99.85%, FAR/FRR: 0.1/0.83
Ma, 2003 [91]	2255 images	99.43%, FAR/FRR: 0.1/0.97
Ma, 2004 [93]	2255 images	99.60%, EER: 0.29%
Ma, 2004 [92]	2255 images	100%, EER: 0.07%
Monro, 2007 [102]	2156 CASIA images and 2955 U. of Bath images	100%
Proenca, 2007 [122]	800 ICE images	EER: 1.03%
Rossant, 2005 [129]	149 images	100%
Rydgren, 2004 [131]	82 images	100%
Sanchez-Reillo, 2001 [136]	200+ images	98.3%, EER: 3.6%
Son, 2004 [141]	1200 images, (600 used for training)	99.4%
Sun, 2004 [144,146]	2255 images	100%
Takano, 2004 [150]	Images from 10 people	FAR/FRR: 0%/26%
Thornton, 2006 [154]	CMU database, 2000+ images	EER: 0.23
Thornton, 2007 [155]	CMU database, 2000+ images	EER: 0.39%
Tisse, 2002 [158]	300+ images	FAR/FRR: 0%/11%
Yu, 2006 [181]	1016 images	99.74%

Under good
conditions the
performance is
up to 99%

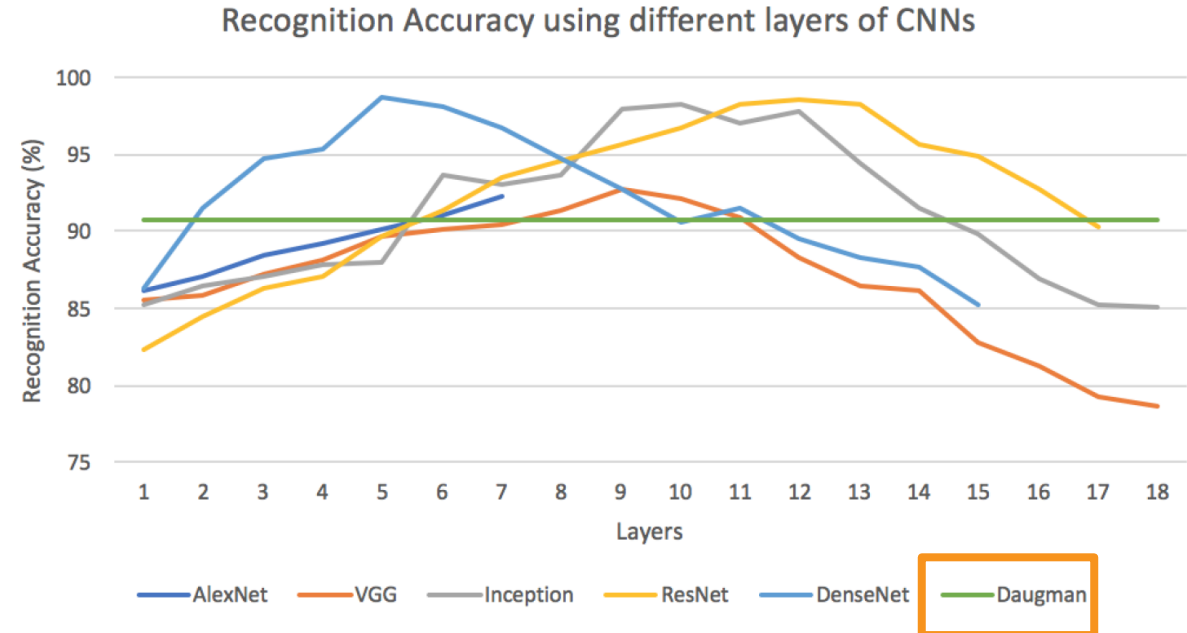
Matching

Using deep learning techniques.

- Feature extraction: CNN popular architectures pre-trained with ImageNet (no transfer-learning).
- Classifier: SVM.



LG2200 database



CASIA-Iris-Thousand

Matching

Using deep learning techniques: Capsule Networks.

TABLE 4. Comparisons of different networks on the JluV3.1 dataset.

Network Structure	LR	Accuracy%	EER%
VGG16_4blocks+DRDL	0.00001	98.43	0.31
VGG16_5blocks+DRDL	0.00001	98.82	0.42
ResNet50_8blocks+DRDL	0.0005	57.25	17.79
ResNet50_9blocks+DRDL	0.0005	62.75	14.46
ResNet50_10blocks+DRDL	0.0005	83.53	6.91
ResNet50_11blocks+DRDL	0.0005	92.16	4.91
ResNet50_12blocks+DRDL	0.0005	96.47	2.83
ResNet50_13blocks+DRDL	0.0005	69.02	15.8
ResNet50_14blocks+DRDL	0.0005	98.04	0.51
ResNet50_15blocks+DRDL	0.0005	99.22	0.078
ResNet50_16blocks+DRDL	0.0005	98.82	0.64
InceptionV3_1block+DRDL	0.00002	89.02	6.3
InceptionV3_3blocks+DRDL	0.00002	81.96	8.46
InceptionV3_4blocks+DRDL	0.00002	98.04	0.89
InceptionV3_5blocks+DRDL	0.00002	99.37	0.039
InceptionV3_6blocks+DRDL	0.00002	98.83	0.21
InceptionV3_7blocks+DRDL	0.00002	98.43	0.45
InceptionV3_8blocks+DRDL	0.00002	97.25	1.7
InceptionV3_9blocks+DRDL	0.00002	97.27	0.78
InceptionV3_10blocks+DRDL	0.00002	85.88	5.31
InceptionV3_11blocks+DRDL	0.00002	72.94	11.36
Iris-Dense+DRDL	0.00001	97.26	1.55
Iris-Inception+DRDL	0.00001	97.65	0.9
Iris-SE+DRDL	0.00001	94.51	1.8
Daugman	—	95.7	2.48
DenseNet_6layers+SVM	—	97.8	2.09
non-seg+nonnorm+ResNet50	0.001	97.93	0.32

TABLE 5. Comparisons of different networks on the JluV4 dataset.

Network Structure	LR	Accuracy%	EER%
VGG16_4blocks+DRDL	0.00001	98.12	0.998
VGG16_5blocks+DRDL	0.00001	98.52	0.65
ResNet50_8blocks+DRDL	0.00001	97.75	0.76
ResNet50_9blocks+DRDL	0.00001	95.33	1.02
ResNet50_10blocks+DRDL	0.00001	95.31	1
ResNet50_11blocks+DRDL	0.00001	97.06	1.13
ResNet50_12blocks+DRDL	0.00001	96.87	1.1
ResNet50_14blocks+DRDL	0.00001	95.23	1.84
ResNet50_15blocks+DRDL	0.00001	94.75	2.16
ResNet50_16blocks+DRDL	0.00001	92.46	3.27
InceptionV3_1block+DRDL	0.00001	98.79	0.35
InceptionV3_2blocks+DRDL	0.00001	95.25	1.33
InceptionV3_3blocks+DRDL	0.00001	97.56	1.13
InceptionV3_4blocks+DRDL	0.00001	98.88	0.295
InceptionV3_5blocks+DRDL	0.00001	98.15	0.67
InceptionV3_6blocks+DRDL	0.00001	98.60	0.84
InceptionV3_7blocks+DRDL	0.00001	97.81	1.42
InceptionV3_8blocks+DRDL	0.00001	94.15	3.55
InceptionV3_9blocks+DRDL	0.00001	93.96	3.49
InceptionV3_10blocks+DRDL	0.00001	80.35	8.15
InceptionV3_11blocks+DRDL	0.00001	67.98	13.54
Iris-Dense+DRDL	0.001	99.42	0.13
Iris-Inception+DRDL	0.001	99.38	0.11
Iris-SE+DRDL	0.001	99.04	0.39
Daugman	—	98.6	0.69
DenseNet_6layers+SVM	—	96.97	2.59
non-seg+nonnorm+ResNet50	0.001	99.14	0.15

Key Challenges

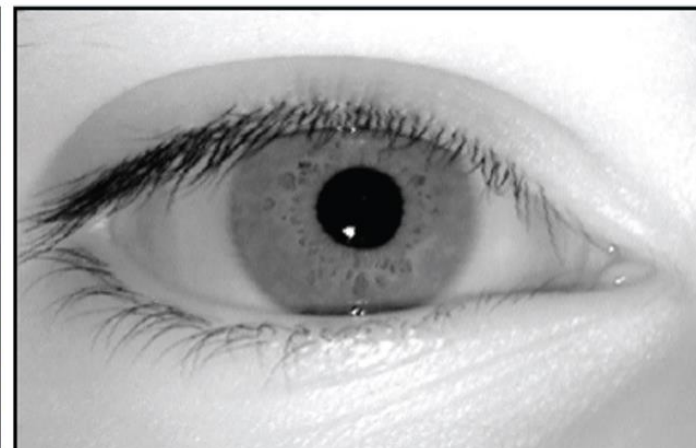
How well can iris recognition be done with [little or no explicit user cooperation?](#)



How well can iris recognition be done using [visible light or cross-wavelength images?](#)



Iris in visible light



Iris in NIR

Long-Range Iris Sensors

Iris recognition systems that operate at longer standoff distances ranging from 1 m to 60 m. Such long range iris acquisition and recognition systems can provide [high user convenience and improved throughput](#).



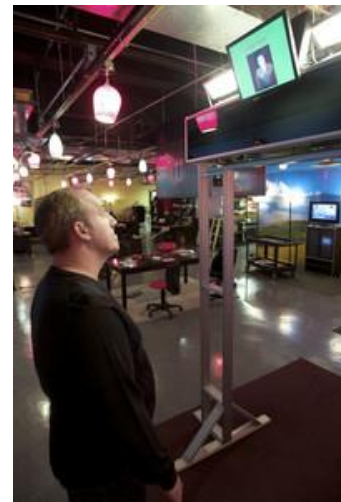
SRI: IOM



SRI: IOM Walk Thru



AOptix Insight



HBox



Cylab

Current distance: max 10 m!

Long-Range Iris Sensors

Iris recognition systems that operate at longer standoff distances ranging from 1 m to 60 m. Such long range iris acquisition and recognition systems can provide [high user convenience and improved throughput](#).



Key References

- K. W. Bowyer and M. J. Burge, *Handbook of iris recognition*. Springer London, 2016.
- J. Daugman, "How iris recognition works," *IEEE Transactions on Circuits and Systems for Video Technology*, 2004.
- A. K. Jain, K. Nandakumar, and A. Ross, "50 years of biometric research: Accomplishments, challenges, and opportunities." *Pattern Recognition Letters*, 79, 80-105, 2016.
- M. De Marsico, A. Petrosino and S. Ricciardi, "Iris recognition through machine learning techniques: A survey," *Pattern Recognition Letters*, 82, 106-115, 2016.
- A. Boyd, Z. Fang, A. Czajka and K.W. Bowyer, "Iris presentation attack detection: Where are we now?," *Pattern Recognition Letters*, 138, 483-489, 2020.
- D. Yadav, N. Kohli, A. Agarwal, M. Vatsa, R. Singh and A. Noore "Fusion of handcrafted and deep learning features for large-scale multiple iris presentation attack detection," in Proc. IEEE Conference on Computer Vision and Pattern Recognition Workshops, 2018.
- C. Wang, Y. Zhu, Y. Liu, R. He and Z. Sun, "Joint iris segmentation and localization using deep multi-task learning framework," arXiv:1901.11195, 2019.
- K. Nguyen, C. Fookes, A. Ross and S. Sridharan, "Iris recognition with off-the-shelf CNN features: A deep learning perspective," *IEEE Access*, 6, 18848-18855, 2017.
- T. Zhao, Y. Liu, G. Huo and X. Zhu, "A deep learning iris recognition method based on capsule network architecture," *IEEE Access*, 7, 49691-49701, 2019.
- M. Arsalan, H. G. Hong, et al., "Deep learning-based iris segmentation for iris recognition in visible light environment," *Symmetry*, 9(11), 263, 2017.
- K. Nguyen, C. Fookes, R. Jillela, S. Sridharan, and A. Ross, "Long range iris recognition: A survey," *Pattern Recognition*, 72, 123-143, 2017.

Iris Recognition

Part of the content is based on the tutorial by Kevin W. Bowyer



BiDA Lab

Biometrics & Data Pattern Analytics Lab

UAM

Universidad Autónoma
de Madrid